NASA CR-954

PANEL LOSS FACTORS DUE TO GAS-PUMPING AT STRUCTURAL JOINTS

By G. Maidanik and E. E. Ungar

Issued by Originator as Report No. 1475

Prepared under Contract No. NAS 5-9694 by
BOLT BERANEK AND NEWMAN INC.
Cambridge, Mass.

for Goddard Space Flight Center

NATIONAL AERONAUTICS AND SPACE ADMINISTRATION

For sale by the Clearinghouse for Federal Scientific and Technical Information
Springfield, Virginia 22151 – CFSTI price $3.00

PANEL LOSS FACTORS DUE TO GAS-PUMPING AT STRUCTURAL JOINTS

By G. Maidanik and E. E. Ungar

ABSTRACT

The recently observed fact that the high-frequency structural damping due to riveted joints is associated with "gas-pumping" in the space between overlapping surfaces is subjected to theoretical and experimental study. A theory is developed, which attributes the damping of plates with riveted-on beams to viscous losses associated with the tangential gas motions in the beam-plate interspace that are generated by normal relative motions of the adjacent beam and plate surfaces. Reasonable agreement is found between theoretical predictions and experimental data obtained for three different gases over a wide range of pressures.

TABLE OF CONTENTS

	Page
ABSTRACT	iii
LIST OF FIGURES	vii
INTRODUCTION	1
THEORETICAL DEVELOPMENT	3
Loss Factor and System Energy	3
Power Dissipation in Interspace Gas	4
Gas Velocity Distribution	5
Effect of Oscillation Boundary Layer Thickness	8
Interaction of Interspace Gas and Structural Motions	10
Effect of Rivets on Plate Motion	10
Effect of Gas on Plate Motion	11
Effect of Plate Motion on Gas Pressure	13
Results	16
Loss Factor in Terms of Gas and Structure Parameters	16
Physical Interpretation	17
Dependence of Gas Viscosity on Gap Thickness	19
Summary	21
EXPERIMENTAL STUDY	23
Measurements	23
Apparatus and Instrumentation	23
Auxiliary Measurements	24
Gap Thickness	24
Acoustic Effects of Vacuum Chamber Volume	25
Loss Factor Contribution Due to Gas Pumping	26

TABLE OF CONTENTS (Cont'd)

	Page
Comparison of Theoretical and Experimental Results	26
Gas Properties	26
Calculations	27
The Transition Parameter B	27
Theoretically Predicted Loss Factor of Test Panel; Experimental Data	29
Discussion	
Agreement Between Theory and Experiment	30
Similarity of Results for Different Gases	31
SUMMARY AND CONCLUSIONS	33
Summary	33
Concluding Remarks	34
Acknowledgement	36
REFERENCES	37
FIGURES	39

LIST OF FIGURES

Figure 1 Plate with multi-point-fastened attached beam.

Figure 2 Geometry and coordinates of section taken through plate, perpendicular to beam length.

Figure 3 The function $H_{\_}(\theta)$.

Figure 4 Test panel.

Figure 5 Dependence of Theoretical Gas-pumping loss factor on transition parameter B.

Figure 6 Gas-pumping loss factor of test panel in air
a) at 250 and 4,000 cps
b) at 500 and 8,000 cps
c) at 1,000 and 16,000 cps
d) at 2,000 and 32,000 cps

Figure 7 Gas-pumping loss factor of test panel in helium
a) at 250 and 4,000 cps
b) at 500 and 8,000 cps
c) at 1,000 and 16,000 cps
d) at 2,000 and 32,000 cps

Figure 8 Gas-pumping loss factor of test panel in Freon 114
a) at 250 and 4,000 cps
b) at 500 and 8,000 cps
c) at 1,000 and 16,000 cps
d) at 2,000 and 32,000 cps

Figure 9 Gas-pumping loss factor of test panel in three different gases
a) at 1,000 cps
b) at 8,000 cps

INTRODUCTION

In a recent study of energy dissipation at riveted structural joints[1,2] it was found that the "gas pumping," which results as adjacent surfaces move toward and away from each other, may contribute significantly to the total damping. This report develops a theory which accounts for this gas-pumping damping and which reveals the effects of various parameters on this damping.

The specific structural configuration analyzed here consists of a plate to which a beam is attached by means of rivets or similar point-connectors (Fig. 1). This type of configuration corresponds to that which has previously been studied experimentally; also, information obtained for such configurations may readily be applied to more complex realistic panel structures.[2]

The theory developed in the present report ascribes the dissipation of energy in the air-pumping process to viscous losses associated with air flow tangential to the beam and plate surfaces, where this air flow is due to pressure gradients that occur in the space between these surfaces as these surfaces move toward and away from each other. The analytical approach taken here is based in part on the work of Dimeff, Lane, and Coon[3], who studied a pressure gage in which the pressure of a gas is inferred from the measured energy that is transferred from a vibrating diaphragm to the gas (and dissipated by the gas). These authors, however, dealt with a simple structure whose motion could be analyzed precisely, whereas the plate-beam system is more complex and does not readily lend itself to precise analysis.

The present study confines itself to vibrations at relatively high frequencies – that is, to frequencies at which the length of a plate bending wave is smaller than the spacing between

adjacent rivets. The reason for the choice of this frequency range is two-fold: (1) the gas pumping damping effect has been found to be most pronounced at these high frequencies, and (2) the analyses for the high-frequency case are in some respects more complex than those for lower frequencies, so that the methodology developed here should facilitate greatly the treatment of corresponding low-frequency problems.

This report is divided into two major sections. The first outlines the theoretical development of an expression for the contribution to the panel loss factor that is made by gas pumping, whereas the second presents corresponding experimental measurements and compares them with theoretical predictions. A summary and recommendations for further work appear at the end of this report.

THEORETICAL DEVELOPMENT

Loss Factor and System Energy

The loss factor of a vibrating system is a convenient measure of its damping. For lightly damped systems vibrating in steady state at circular frequency ω the loss factor η may be defined as

$$\eta = \Phi_a / \omega E \quad , \tag{1}$$

where Φ_a denotes the time-average rate of energy dissipation (that is, the average power dissipated) and E denotes the total energy of the vibrating system.[4]

The system energy E may be calculated readily if the system's mass and velocity distributions are known. The latter may be visualized with the aid of Fig. 2, which represents a section taken through the plate-and-beam system perpendicular to the beam length. For sinusoidal time-dependences, as are assumed throughout this derivation, one may represent any time-varying quantity v as

$$v(x,y,t) = \mathrm{Re}\left[V(x,y)\ e^{i\omega t} \right] \quad , \tag{2}$$

where the quantity V(x,y) is complex in general, and is known as a phasor.* Then, if V_p is the phasor which represents the velocity (due to flexure) everywhere on the plate, except at and near that region which is covered by the beam, if V_s is the velocity phasor

*Throughout this report, capital letters are used to represent phasors which pertain to time-varying quantities represented by the corresponding lower case letters.

for the beam-covered region, and if V_b is the velocity phasor for the beam itself, one may express the energy E_s in the plate-and-beam system as

$$E \approx (A_p - A_b)\, m_p \langle |V_p|^2 \rangle + A_b \left[m_p \langle |V_s|^2 \rangle + m_b \langle |V_b|^2 \rangle \right]$$

$$\approx A_p m_p \langle |V_p|^2 \rangle \quad . \tag{3}$$

Here A_p denotes the total plate surface area (one side), A_b denotes the total beam surface area that is "in contact" with the plate, and m_p and m_b represent the plate and beam masses per unit area; the brackets $\langle\ \rangle$ indicate spatial (x,y) averages of the quantities they enclose. The second approximate equality of Eq. (3) applies for the usual case where the plate area is much greater than the beam area, and where the mean-square plate velocity $\langle |V_p|^2 \rangle$ in the plate region that is not covered by the beam greatly exceeds both the plate mean-square velocity $\langle |V_s|^2 \rangle$ in the beam-covered plate strip and the mean-square velocity $\langle |V_b|^2 \rangle$ of the beam itself.

Power Dissipation in Interspace Gas

In addition to the energy E of the vibrating system, one must know the time-average power dissipation Φ_a if one desires to determine the system loss factor according to Eq. (1). This time-average power may be calculated from the instantaneous rate of energy dissipation Φ. For a volume U of an incompressible fluid, this rate of enery dissipation is given by [5]

$$\Phi = 2\mu \int_U \left[\sum_{r=x,y,z} \sum_{s=x,y,z} \left(\frac{\partial v_r}{\partial s} \right)^2 \right] dU \quad , \qquad (4)$$

where μ denotes the fluid's viscosity, and $v_r = v_r(x,y,z,t)$, $r = x,y,z$, denotes the component of the fluid velocity parallel to the r-coordinate. Since in all practical cases of interest here the velocities are small compared to the velocity of sound, and since a gas behaves essentially as if it were incompressible for such velocities, the foregoing equation may also be applied here for the gas that occupies the space between the beam and the plate.

For the present case, where all quantities vary sinusoidally with time, one may introduce phasors and express the time-average value of the power dissipated as

$$\Phi_a = \mu \int_U \left[\sum_{r=x,y,z} \sum_{s=x,y,z} \frac{\partial V_r}{\partial s} \frac{\partial V_r^*}{\partial s} \right] dU \quad , \qquad (5)$$

where the asterisk denotes the complex conjugate of the quantity to which it is attached.

Gas Velocity Distribution

In order to determine the velocity distribution that describes the motion of the air in the beam-plate interspace, one requires the equation of a motion of viscous fluids (that is, the Navier-Stokes equation),[5]

$$\rho \frac{\partial \underset{\sim}{v}}{\partial t} + (\underset{\sim}{v} \cdot \underset{\sim}{\text{grad}})\underset{\sim}{v} = - \underset{\sim}{\text{grad}}\ p + \mu \nabla^2 \underset{\sim}{v} + (\zeta + \tfrac{\mu}{3})\ \text{grad div}\ \underset{\sim}{v} \qquad (6)$$

and the equation of continuity[5]

$$\frac{\partial \rho}{\partial t} + \rho\ \text{div}\ \underset{\sim}{v} + \underset{\sim}{v} \cdot \underset{\sim}{\text{grad}}\ \rho = 0 \qquad . \qquad (7)$$

Here ρ denotes the fluid density, ζ the "second viscosity," and $\underset{\sim}{v}$ represents the fluid velocity vector (which has components v_x, v_y, v_z). Tildes (~) are used to designate vectors and vector-like quantities.

For flows involving small Mach numbers, the fluid may be regarded as incompressible, as pointed out previously, and for incompressible fluids $\underset{\sim}{\text{grad}}\ \rho = 0$. The $\partial\rho/\partial t$ term in Eq. (7) may also be neglected if the time taken by a small disturbance to traverse a characteristic length is small compared to the time during which the flow changes appreciably.[5] Under these conditions Eq. (7) implies div $\underset{\sim}{v}$ = 0, and Eq. (6) may be simplified accordingly. For small Reynolds numbers the $(\underset{\sim}{v} \cdot \underset{\sim}{\text{grad}})\ \underset{\sim}{v}$ term may also be neglected,[5] and Eq. (6) reduces to

$$\rho \frac{\partial \underset{\sim}{v}}{\partial t} = - \underset{\sim}{\text{grad}}\ p + \mu\ \nabla^2\ \underset{\sim}{v} \qquad . \qquad (8)$$

If one assumes the velocity vector $\underset{\sim}{v}$ and the pressure p to vary sinusoidally in the x and y directions (parallel to the plane of the plate, see Fig. 2) and in time, then one may write

$$\underset{\sim}{v}(x,y,z,t) = \mathrm{Re}\left[\underset{\sim}{V}(x,y,z)e^{i\omega t}\right] , \qquad \underset{\sim}{V}(x,y,z) \equiv \underset{\sim}{W}(z)e^{-i(k_x x+k_y y)} \tag{9}$$

$$\underset{\sim}{\text{grad } p} = \mathrm{Re}\left[\underset{\sim}{(\text{GRAD } p)}e^{i\omega t}\right] , \qquad \underset{\sim}{(\text{GRAD } p)} \equiv \underset{\sim}{Q}(z)\, e^{-i(k_x x+k_y y)} .$$

Substitution of Eq. (9) into (8) yields

$$\frac{d^2}{dz^2}\underset{\sim}{W}(z) - \left(\frac{i\omega\rho}{\mu} + k_x^2 + k_y^2\right)\underset{\sim}{W}(z) = \frac{\underset{\sim}{Q}(z)}{\mu} . \tag{10}$$

This differential equation may readily be solved by standard techniques. If the pressure gradient is independent of the z-coordinate, so that $\underset{\sim}{Q}(z)$ is a vector whose components are complex constants, one finds upon use of the boundary conditions $v_x(\pm h/2) = v_y(\pm h/2) = 0$ that

$$\frac{W_x(z)}{Q_x} = \frac{W_y(z)}{Q_y} = \frac{1}{-s^2\mu}\left[1 - \frac{\cos(sz)}{\cos(sh/2)}\right] , \tag{11}$$

$$s^2 \equiv -\left(k_x^2 + k_y^2 + i\omega\rho/\mu\right) = -\left(k_x^2 + k_y^2 + 2i/\delta^2\right) .$$

The symbol δ which was introduced above, denotes the effective depth of penetration of an oscillatory disturbance, or the "oscillation boundary layer thickness," which is given by[5]

$$\delta = \sqrt{2\mu/\rho\omega} = \sqrt{2\nu/\omega} . \tag{12}$$

Here $\nu=\mu/\rho$ represents the kinematic viscosity of the fluid.

Effect of Oscillation Boundary Layer Thickness

By use of Eq. (9) one may reduce the integrand of Eq. (5) to

$$\sum_{r,s\,=\,x,y,z}\sum \frac{\partial V_r}{\partial s}\cdot\frac{\partial V_r^*}{\partial s} = \sum_{r=x,y,z}\left[\left(\frac{dW_r}{dz}\right)\left(\frac{dW_r}{dz}\right)^* + \left(k_x^2+k_y^2\right)\left|W_r\right|\left|W_r\right|^*\right] . \tag{13}$$

For the case of interest at present, the wavelengths in the x-y plane greatly exceed the plate separation h; then $h\sqrt{k_x^2+k_y^2} \ll 1$ and one may neglect the last set of terms of Eq. (13). By substituting Eqs. (11) and (13) into (5) and neglecting the small z-velocity contributions one may then obtain

$$\Phi_a = \frac{||\,\underset{\sim}{Q}\,(z)\,||^2\,A_b}{\mu\,|s|^2}\int_{-h/2}^{h/2}\left|\frac{\sin(sz)}{\sin(sh/2)}\right|^2 dz \quad , \tag{14}$$

where integration indicated in Eq. (5) is carried out over the volume $U=A_b h$ of the beam-plate interspace, and where

$$||\underset{\sim}{Q}(z)||^2 \equiv |Q_x|^2 + |Q_y|^2 + |Q_z|^2 \quad , \tag{15}$$

has been defined, so that $||\underset{\sim}{Q}(z)||$ represents the length of a vector whose components are the absolute values of the complex numbers which represent the components of the $\underset{\sim}{Q}(z)$ vector.

For the case which is of primary interest here the wavelengths in the x-y plane greatly exceed the oscillatory boundary layer thickness δ, as well as the separation h. Therefore, $\delta\sqrt{k_x^2+k_y^2} \ll 1$ here and $s \approx \pm (1-i)/\delta$. With this approximation one may readily carry out the integration indicated in Eq. (14) to obtain a result which one may express as

$$\Phi_a = \frac{A_b h}{\rho\omega} \left|\left|\underset{\sim}{Q}(z)\right|\right|^2 H_-(\theta) \quad , \tag{16}$$

where

$$H_-(\theta) \equiv \frac{\sinh(\theta) - \sin(\theta)}{(\theta)\,[\cosh(\theta) + \cos(\theta)]}$$

$$\theta \equiv h/\delta \quad , \tag{17}$$

and where Eq. (12) has been used to eliminate μ.

The function $H_-(\theta)$, which embodies the effect of the oscillation boundary layer thickness δ on the power dissipation, is plotted in Fig. 3. A discussion of the meaning and the implications of the shape of this curve appears in a later section of this report.

In the foregoing it has tacitly been assumed that edge effects are negligible; i.e., that the fluid behavior near the beam edges, which differs from that of the bulk of the fluid, does not affect the total power Φ_a significantly. This assumption is valid as long as the separation h between the adjacent beam and plate surfaces is small in comparison to any linear dimension of the overlapping areas.

Now, having obtained Eq. (16), one may use it and Eq. (3) in Eq. (1), to find the following expression for the loss factor:

$$\eta \approx \frac{A_b\, h}{A_p\, m_p \rho \omega^2} \frac{||\underset{\sim}{Q}(z)||^2}{\langle |V_p|^2 \rangle} H_-(\theta) \quad . \tag{18}$$

One still requires a relation between the plate velocity V_p and the interspace gas pressure p in order to evaluate Eq. (18) fully. The subsequent sections are addressed to the derivation of such a relation.

Interaction of Interspace Gas and Structural Motions

In order to determine the pressure gradient that exists in the beam-plate interspace, one must analyze how the interspace pressure and the structural motions interact. The plate velocity distribution v_s in the region covered by the beam may be expected to differ from the velocity field v_p on the remainder of the plate, because of the beam, which acts on the plate both via the mechanical fasteners (e.g., rivets) and via the gas that occupies the space between the adjacent beam and plate surfaces. The pressure in the interspace, of course, depends directly on the structural motions.

Effect of Rivets on Plate Motion

The effect of a rivet on the plate velocity field is, in essence, confined to a circular region with radius k_p^{-1} around the rivet.[1] A row of rivets, in which the spacing between rivets encompasses many plate flexural wavelengths, may thus be expected to have little effect on the average velocity of the beam-covered portion of the plate. The effect of a row of rivets in producing a velocity field v_s in the beam-covered portion of the plate when there exists a velocity field v_p on the remainder of the plate may be summarized by the expression

$$\langle|V_s|^2\rangle = \langle|V_p|^2\rangle\, S(k_p d) \quad , \tag{19}$$

where d denotes the distance between adjacent rivets. $S(k_p d) \approx 1$ for $k_p d \gtrsim 5$, but for smaller values of the argument $S(k_p d)$ is a complicated function which exhibits peaks for $2k_p d \approx 1,2,3, \ldots$ [1]

The effect of the gas in the interspace on the motion of the beam-covered plate strip is superposed on that of the rivets. Unfortunately, the rivet effect is associated with the point impedance of the plate, whereas the gas effect (as discussed subsequently) is associated essentially with the line impedance of the plate. The dependences on these two types of impedance lead to great analytical complications — and, in order to avoid these, it is convenient to assume that the two effects are uncorrelated. Use of this assumption prevents one from accounting for some of the details of the plate motion, such as resonances and antiresonances that may occur between the two effects, but it makes analysis of the gross properties feasible and should yield good results at least for $k_p d > 5$.

Effect of Gas on Plate Motion

In order to analyze the effect of the interspace gas pressure on the plate motion most simply, one may take note of the fact that the beams (or other reinforcing or supporting members) in most practical structural configurations are much longer than they are wide. Plate waves thus impinge on a beam primarily laterally, so that the wave propagation on the plate in the vicinity of the beam will on the average be predominantly in the x-direction (perpendicular to the beam length).[6] An "average" wave motion on the beam-covered plate strip thus is independent of the y-coordinate

(measured parallel to the beam length) and is governed by a wavenumber $k_x = k_p$ in the x-coordinate direction.

The response of a plate to such a pressure distribution is governed by the plate's "line impedance;" i.e., by the impedance of the plate to a force which is uniformly distributed along a straight line. However, the pressure distribution on the plate strip is composed of an infinitude of parallel line forces (and the magnitudes of these forces have the same spatial and temporal periodicity as the plate waves), so that the velocity at each point on the plate strip depends not only on the pressure (line force) that acts directly at that point, but on the forces that act on the entire strip.

The matching of the periodicities of the forces and of the plate waves causes the velocity at each point to be greater than that produced by an independently acting line force. One may account for this increased velocity either by introducing an effective impedance which is smaller than the line impedance, or by introducing an increased artificial "effective" pressure P_e whose use in conjunction with the line impedance results in the correct plate velocity. One finds that

$$P_e = \beta P_a \quad , \quad \beta \approx 1 + k_p b/\pi \quad , \tag{20}$$

where b denotes the beam width and P_a the acoustic pressure (i.e., the change from ambient pressure).

The validity of the above expression for β may readily be verified. The term $k_p b/\pi$ represents the number of half-wavelengths of the pressure field (associated with the plate velocity field) that extend over the beam and plate strip width b. Since the periodicities of the pressure and plate velocity fields are the same, the pressures acting at points separated by an integral number of half-wavelengths make in-phase contributions to the velocity at any single point. Thus, the effective pressure at any point exceeds the actual pressure by the number of half-wavelengths over which the pressure field extends. (The contributions from points with other than integral multiples of half-wavelength spacing essentially cancel each other, on the average.)

The action of the interspace pressure produces a change in the plate velocity from v_p (outside the beam-covered strip) to v_s (on the strip). One may thus write

$$\beta P_a = - Z(V_s - V_p) \quad , \tag{21}$$

where Z denotes the line pressure impedance of the plate and is given by

$$Z = 4\omega m_p/(1-i) \tag{22}$$

in terms of the mass m_p per unit area of the plate.[8]

Effect of Plate Motion on Gas Pressure

In order to obtain a second relation between P_a and V_s, so that one then can eliminate V_s from Eq. (21), one may turn to the equation of continuity, Eq. (7). As previously mentioned,

grad p ≈ 0 here, in view of the small Mach numbers involved. From the equation of state of an ideal gas,

$$p\rho^{-\gamma} = \text{constant} \quad , \tag{23}$$

where γ is a suitable "polytropic" exponent,* one may deduce that

$$\frac{1}{\rho}\frac{\partial \rho}{\partial t} \approx \frac{1}{\gamma p_o}\frac{\partial p_a}{\partial t} \quad , \tag{24}$$

where p_o denotes the average (ambient) gas pressure. Eq. (7) then may be rewritten as

$$\frac{1}{\gamma p_o}\frac{\partial p_a}{\partial t} + \frac{\partial v_x}{\partial x} + \frac{\partial v_y}{\partial y} + \frac{\partial v_z}{\partial z} = 0 \quad . \tag{25}$$

Since in the beam-covered region the wave propagation is essentially independent of y, as previously discussed, one may introduce phasors as indicated in Eqs. (9) and write

$$\frac{p_a}{P_a} = \frac{\mathcal{V}}{\mathcal{W}} = \frac{v_s}{V_s} = e^{i(\omega t - k_p x)} \quad , \tag{26}$$

where taking of the real part is implied, of course. Introduction of these phasors into Eq. (25) yields

*This exponent depends on the thermodynamic process that the gas undergoes. For isothermal processes $\gamma = 1$; for reversible adiabatic, or "isentropic," processes, γ is equal to the ratio of specific heats.

$$\frac{i\omega P_a}{\gamma p_o} - ik_p W_x + \frac{dW_z}{dz} = 0 \quad , \tag{27}$$

and integration of this result over the gap leads to

$$\frac{i\omega P_a h}{\gamma p_o} - ik_p \int_{-h/2}^{h/2} W_x \, dz = - W_z \Big]_{-h/2}^{h/2} = V_s \quad . \tag{28}$$

In the foregoing, the pressure has been taken as independent of z, as is reasonable for the generally satisfied condition $k_o h \ll 1$, where k_o denotes the acoustic wavenumber; the gas velocity in the z-direction has been taken as zero at $z = h/2$ (since the beam velocity $v_b \approx 0$) and as v_s at $z = -h/2$.

One may evaluate the integral appearing in Eq. (28) by using the expression of Eq. (11) for W_x and the previously employed approximation $s \approx (1+i)/\delta$. For p_a as given by Eq. (26) one finds that $(\text{GRAD } p)_x = -ik_p P_a$ here, and that

$$\int_{-h/2}^{h/2} W_x(z) dz = \frac{-hk_p P_a \delta^2}{2\mu} [1 - H_+(\theta) - iH_-(\theta)] \quad , \tag{29}$$

where $H_-(\theta)$ and $\theta = h/\delta$ are defined in Eqs. (17) and $H_+(\theta)$ is analogously defined as

$$H_+(\theta) = \frac{\sinh(\theta) + \sin(\theta)}{\theta[\cosh(\theta) + \cos(\theta)]} \quad . \tag{30}$$

If one substitutes Eq. (28) into Eq. (21) and solves for V_p in terms of P_a one obtains

$$R \equiv \frac{V_p}{P_a} = \frac{\beta(1-i)}{4\omega m_p} + \frac{k_p^2 h}{\rho\omega}\{H_-(\theta) + i[1 - H_+(\theta)]\} + \frac{i\omega h}{\gamma p_o} \qquad (31)$$

with the aid of Eqs. (12) and (22).

Results

Loss Factor in Terms of Gas and Structure Parameters

If one determines $\underset{\sim}{Q}(z)$ by calculating grad p from Eq. (26) and comparing the result to the corresponding expression of Eq. (9), then one finds by applying Eq. (26) that here $||\underset{\sim}{Q}(z)||^2 = k_p^2|P_a|^2$. One may then determine that

$$\frac{||\underset{\sim}{Q}(z)||^2}{<|V_p|^2>} \approx \frac{k_p^2|P_a|^2}{|V_p|^2} = \left|\frac{k_p}{R}\right|^2 \quad , \qquad (32)$$

if one considers that $|V_p|^2 = 2<|V_p|^2>$, but also notes that the foregoing analysis has overestimated the numerator by a factor of 2 (since, on the average, the randomly incident waves cause only half as much dissipative gas motion as the normally incident waves that had been assumed in the analysis).

Substitution of Eqs. (31) and (32) into (18) yields a result which may be expressed as

$$\eta = \left(\frac{A_b}{A_p}\right)\left(\frac{Z_a}{Z_p}\right)\left(\frac{S}{G}\right)\left(\frac{\omega_c}{\omega}\right) H_-(\theta) \quad , \qquad (33)$$

where

$$G \equiv \left[1 + \left(\frac{\omega_c}{\omega}\right)(1-H_+) - \frac{\beta}{4}\left(\frac{Z_a}{Z_p}\right)\right]^2 + \left[\left(\frac{\omega_c}{\omega}\right) H_- + \frac{\beta}{4}\left(\frac{Z_a}{Z_p}\right)\right]^2 \qquad (34)$$

and

$$\begin{aligned} Z_a &= \gamma p_o/\omega h \quad , \quad Z_p = m_p \omega \\ \omega_c/\omega &= (k_p\, c_o/\omega)^2 = \gamma p_o k_p^2/\omega^2 \rho \quad . \end{aligned} \qquad (35)$$

In the foregoing, S represents the absolute value of the function $S(k_p d)$ of Eq. (19), and has been introduced here to account for the effect of the rivets. Introduction of S in this manner is legitimate, in view of the assumption that pressure and rivet effects are uncorrelated.

The symbols defined in Eq. (35) have useful physical interpretations. Z_a may seem to be the absolute value of the stiffness impedance of the gas in the interspace, for unit area (measured parallel to the plate surface). Similarly, Z_p is the absolute value of the inertia impedance of unit area of the plate. The symbol ω_c represents the acoustic critical frequency, i.e. the frequency at which a flexural wave on the plate has the same wavelength as an acoustic wave in the ambient gas.[9]*

Physical Interpretation

The loss factor given by Eq. (33) clearly is independent of the amplitude of the plate vibrations. This independence follows from the proportionality between the plate velocity and gas pressure amplitudes, and from the proportionality between time-average power dissipation and plate vibrational energy implied by this relation between the pressure and velocity amplitudes. Amplitude-independence of the loss factor has also been observed experimentally (in absence of impacts between the beam and plate surfaces) previously[1] and in the experiments the results of which are presented subsequently.

*The relation $c_o^2 = \partial p/\partial \rho = \gamma p_o/\rho$, where c_o denotes the acoustic velocity of the gas, may be obtained from the equation of state, Eq. (23).

Equation (33) shows that the loss factor η associated with air-pumping in the beam-plate interspace in a narrow frequency band[6] centered on ω depends on the ratio A_b/A_p of beam area to plate area, on the ratio Z_a/Z_p of air stiffness impedance to plate mass impedance per unit area, on the ratio ω_c/ω of the acoustic critical frequency to the frequency of interest, on the ratio $\theta = h/\delta$ of the average gap (interspace) thickness to the oscillation boundary layer thickness (via the function H_-) and on S/G. The function S accounts for the effect of the rivets on the plate motion, whereas the function G accounts for the interaction between the gas and plate motions.

The function $H_-(\theta)$, which embodies the dependence of power dissipation on the ratio θ of gap to boundary layer thickness, is plotted in Fig. 3. As evident from this figure or from Eq. (17), $H_-(\theta)$ increases monotonically for small θ, reaches a peak at $\theta \approx 2$, then decreases monotonically. This behavior of $H_-(\theta)$ can readily be explained in physical terms. Large values of $\theta = h/\delta$ correspond to conditions where the boundary layer occupies only a small fraction of the total gap thickness h; since energy dissipation occurs primarily within the boundary layer, this is in effect confined to a small region of the gap, and the damping is small. Small values of h/δ correspond to conditions where the boundary layer thickness is large compared to the gap width. Here the boundary serves to restrict the motion of all of the gas in the interspace, again resulting in small dissipation. The greatest amount of damping occurs at an intermediate value of h/δ, where the boundary layer is thick enough so that most of the gas participates in the dissipation, yet thin enough so as not to restrict the gas motion excessively.

One may also note that the function G depends on the ambient pressure p_o via the impedance ratio Z_a/Z_p. For low pressures (and high enough frequencies, so that $\omega_c/\omega < 1$) G approaches unity, whereas for high pressures G may exceed unity considerably. This behavior of the function G may be ascribed to the fact that at low pressures the gas does not restrict the relative motion between the plate and beam appreciably, whereas at high pressures it does restrict this motion and thus results in decreased gas pumping and corresponding in lesser damping.

It appears that the first bracketed expression of Eq. (34) can vanish under appropriate conditions, which correspond to a resonance between the gas and the beam-covered plate strip. At such a resonance G tends to take on a relatively small value, and the loss factor tends to become relatively large. However, the dissipative terms (the second bracketed expression) ensure that the resonance remains weak— i.e., that G does not become very small. Hence, this resonance should have no appreciable effect on the behavior of the loss factor η.

Dependence of Gas Viscosity on Gap Thickness

The kinematic viscosity ν of a gas is classically given by

$$\nu = C_m \Lambda / 2 \tag{36}$$

in terms of the mean speed C_m of the molecules and the molecular mean free path Λ. The foregoing classical expression, however, applies only if all dimensions of the space to which the gas is confined are greater than the mean free path.

If a gas is confined to a region between two surfaces which are separated by a distant h that is of the order of Λ or smaller, then collisions of the molecules with the surfaces dominate the gas dynamics, rather than intermolecular collisions (which dominate in the classical case). The gap thickness h then affects the mean free path, and therefore the kinematic viscosity. Although there exists no firm theoretical basis for taking this thickness into account, it appears from previous work on a closely related problem[3] that one may reasonably write

$$\nu \approx C_m h/2B \tag{37}$$

for the case where $\Lambda \geq h$. Here B is a dimensionless constant, the value of which must be determined empirically.

It is convenient to "bridge" the expressions of the two foregoing equations mathematically, in order to represent a smooth transition between the large-space and narrow-gap regimes. One may easily verify that the expression

$$\nu = \frac{C_m\, h\, \Lambda}{2(h + B\Lambda)} \tag{38}$$

reduces to Eq. (36) for $h \gg B\Lambda$ and to Eq. (37) for $h \ll B\Lambda$.

Since the molecular mean free path Λ of a gas varies inversely with the pressure p_o one may set $\Lambda = K/p_o$, where K is a constant, and rewrite Eq. (38) explicitely in terms of pressure as

$$\nu = \frac{C_m hK}{2(hp_o + BK)} \quad . \tag{39}$$

Summary

It may be useful now to collect all of the previously derived results, and to present them in a form suitable for calculations. From the foregoing work* one finds that the gas-pumping loss factor η observed in a narrow frequency band centered on ω obeys

$$\eta = \left(\frac{A_b}{A_p}\right)\left(\frac{Z_a}{Z_p}\right)\left(\frac{S}{G}\right)\left(\frac{\omega_c}{\omega}\right) H_-(\theta) \tag{34}$$

where

$$G = \left[1 + \left(\frac{\omega_c}{\omega}\right)(1-H_+) - \frac{\beta}{4}\left(\frac{Z_a}{Z_p}\right)\right]^2 + \left[\left(\frac{\omega_c}{\omega}\right) H_- + \frac{\beta}{4}\left(\frac{Z_a}{Z_p}\right)\right]^2 \tag{35}$$

$$\frac{Z_a}{Z_p} = \frac{\gamma p_o}{m_p h \omega^2} \tag{36a}$$

$$\frac{\omega_c}{\omega} = \left(\frac{k_p c_o}{\omega}\right)^2 = \sqrt{12(1-\sigma^2)}\,\frac{c_o^2}{c_L\,\omega h_p}$$

$$\theta = \left[\frac{h\omega}{C_m}\,B + \left(\frac{h p_o}{K}\right)\right]^{1/2} \tag{40}**$$

---

*Use has also been made of the classical expression for the plate flexural wavenumber

$$k_p^4 = 12(1-\sigma^2)\,(\omega/h_p c_L)^2 \quad , \tag{41}$$

where h_p denotes the plate thickness, c_L the longitudinal wave velocity in the plate material, and σ that material's Poisson's ratio.

**From Eqs. (12), (17), and (39).

$$H_{\pm}(\theta) = \frac{\sinh\theta \pm \sin\theta}{\theta[\cosh\theta + \cos\theta]} \qquad (41)^*$$

$$\beta \approx 1 + \left[\frac{12(1-\sigma^2)}{\pi^4}\left(\frac{\omega b^2}{h_p c_L}\right)^2\right]^{1/4} \qquad (20a)$$

*From Eqs. (17) and (30).

EXPERIMENTAL STUDY

Measurements

A program of experiments was undertaken in order to test the validity of the theory developed in the preceding pages. This program consisted primarily of measuring the damping of a sample plate, with and without a bolted-on beam, at various pressures and in three gases of widely differing kinematic viscosities: air, helium, and "Freon 114".

Apparatus and Instrumentation

A 1/64-inch thick plate of 2024-T3 aluminum was used in the experimental program. The test plate was shaped irregularly, as shown in Fig. 4, in order to facilitate the generation of diffuse flexural wave fields on the plate. The plate material was selected because of its relatively low inherent damping, so that the damping contributions due to the gas pumping could be measured more readily.

A one-inch wide, 1/4-inch thick, aluminum beam was attached to the plate near one edge, as shown in Fig. 4, by means of bolts spaced 3 inches apart. Since previous work[1] had shown that bolt torque, surface roughness, and chemical cleanliness had no significant effect on damping, no attempt was made to keep these parameters within close bounds.

Two thin 1/2-inch diameter PZT-5 piezoelectric discs (Clevite Corporation) were epoxy-bonded to the test plate, at the locations indicated in Fig. 4. These discs served to excite the plate and to sense its vibrations.

The plate-and-beam assembly was suspended by means of fine wire springs from a pedestal, and the entire apparatus was

placed in a 28-inch high, 17-inch diameter cylindrical vacuum chamber. Great care was exercised so that no part of the plate-and-beam assembly touched the pedestal or chamber walls, and fine wire leads were used to connect the PZT discs to the external electronics, in order to introduce as little spurious damping as possible.

A typical experiment consisted of pumping the vacuum chamber down to the desired pressure, then measuring the damping of the test panel over the entire frequency range of interest. A McLeod gage (F.J. Stokes Co., No. 276AA) and an Alphatron Vacuum gage (NRC Equipment Corp.) were used to measure the chamber pressure.

All damping measurements were made by the well-established decay-rate technique.[10] This technique consists of exciting the panel via one of the piezoelectric discs by third-octave-filtered white-noise, then turning off the excitation and observing the rate of decay of the free vibrations (or the time required for the vibration level to decay to a given fraction of its initial value). The electronic instrumentation system that was used here is the same as that described in Ref. 2.

Auxiliary Measurements

Gap Thickness

The average thickness of the gap between adjacent surfaces of the plate and beam is a quantity which has a major effect on the gas-pumping that results in that gap due to motion of the plate relative to the beam. The average gap thickness in the experimental assembly was determined by the simple expedient of measuring (by means of a micrometer) the thickness of the beam by itself, of the plate by itself (in the beam-covered region), and then of the plate-plus-beam assembly. The amount by which

the assembly thickness exceeds the total metal thickness may then be ascribed to the gap which is occupied by gas.

Twenty-one measurements were taken of each thickness, at various points along the beam length. Beam thickness values were found to lie between 0.2507 and 0.2515 inches, plate thickness values between 0.0328 and 0.0330 inches, and assembly thickness values between 0.2839 and 0.2880 inches. The corresponding total metal thickness values were found to range from 0.2835 to 0.2843 inches, leading to calculated gap thickness values between 0.0000 and 0.0042 inches. The average gap thickness was determined to be 0.0016 inches.

Acoustic Effects of Vacuum Chamber Volume

There was some concern that the vibrating test panel might be strongly coupled to some modes of the gas in the chamber, and thus exchange energy with these modes, leading to erroneous damping measurements. Therefore, a series of damping measurements were performed on the test panel outside of the vacuum chamber, as well as inside the vacuum chamber (at atmospheric pressure). No measurable differences were observed; since acoustic effects should be more pronounced at higher pressures, one may conclude that the gas volume in the chamber did not distort the plate damping measurements significantly.

The damping one would expect to obtain due to acoustic radiation from the plate-and-beam assembly was also calculated by means of the reasonably well-validated theory of Ref. 6. The calculated loss factor contributions due to acoustic radiation were found to be at least an order of magnitude smaller than any of the loss factors measured on the bare (beam-less) plate; acoustic radiation, therefore, is expected to have no significant effect on the experimental results.

Loss Factor Contribution Due to Gas Pumping

In order to determine the amount of damping that may be ascribed to gas pumping in the beam-plate interspace, two sets of experiments were performed. In one set, the damping of the plate-and-beam assembly was measured at various frequencies and gas pressures; in the other, the damping of the bare (beam-less) plate was measured under the same conditions.

The damping of the bare plate was found to be independent of gas pressure and of the type of gas in the chamber. Hence, this damping may be ascribed to the plate material, with possibly a small contribution from the support system. The damping of the plate with the beam attached always was found to exceed that observed under the same conditions, but in absence of the beam. The damping increase obtained (over the corresponding bare-plate condition) when the beam is attached is taken to represent the damping contribution due to gas pumping, since all other damping mechanisms that are brought into play when the beam is mounted on the plate are believed to have negligible effects.[1]

Comparison of Theoretical and Experimental Results

Gas Properties

In order to determine the damping effect that the previously discussed theory predicts for a given gas and a given beam-plate configuration, one must know three properties of the gas: (1) the molecular mean free path at a known pressure, (2) the mean molecular velocity at a known temperature, and (3) the acoustic velocity at a known temperature. [The mean free path is independent of temperature, and the molecular and acoustic velocities do not depend significantly on pressure.[11]]

Values of these three properties cannot readily be found from the literature, but may be calculated from other, more easily found values by use of relations available from gas dynamics theory.[11] Table I lists data on the three gases used in the experimental program, including the calculated values of the three aforementioned properties, and also indicates how these were calculated. The range of kinematic viscosities covered is of particular interest here; the kinematic viscosity of helium is about 5 times that of air, and that of air is nearly 7 times that of Freon 114.

Calculations

Calculations were performed for the test plate-and-beam system, based on the previously presented theoretical expressions, on the gas property values listed in Table I, and using a gap thickness $h=2\times10^{-3}$ in $\approx 5\times10^{-3}$ cm. (This gap thickness value represents the average measured value correct to one significant figure. The accuracy of the measurements does not warrant the use of more figures. Calculations indicate that the results are not significantly changed by changes in the value of h.)

The Transition Parameter B.

Initially some exploratory calculations were undertaken to determine what value of the parameter B will result in the best agreement between theory and experiment. A typical set of curves, showing how the theoretically predicted air-pumping loss factor varies with pressure, for several values of B, appears in Fig. 5. Higher values of B are seen to result in generally greater loss factor values, in more pronounced peaks, and in lesser slopes at

TABLE I - PROPERTIES OF GASES

			Air	Helium	Freon 114
v	Specific volume[a,b] $=1/\rho$	(ft^3/lb)	18.4[12]	102.[12]	2.3[14]
		(cm^3/gm)	1150.	6380.	144.
γ	Ratio of Specific Heats		1.40[12]	1.67[12]	1.08[14]
c_m	Mean Molecular Velocity[b] $=1.66\sqrt{p/\rho}$ [11]	(10^4in/sec)	1.8	4.9	0.75
		(10^4cm/sec)	4.6	12.5	1.9
c_o	Acoustic Velocity[b] $=\sqrt{\gamma p/\rho}$ [11]	(10^4in/sec)	1.35	4.0	0.49
		(10^4cm/sec)	3.4[11]	10.	1.25
μ	Viscosity[a,b]	(centipoises)	0.018[13]	0.018[13]	0.011[14]
		(10^{-5}lb/sec ft)	1.2	1.2	.74
		(10^{-4}gm/sec cm)	1.8	1.8	1.1
ν	Kinematic viscosity[a,b] $=\mu v$	($10^{-5}ft^2/sec$)	22.	120.	1.8
		(cm^2/sec)	.21	1.15	.016
Λ	Molecular Mean Free Path[a,b] $=2\nu/c_m$	(10^{-6}in)	2.3	6.9	0.71
		(10^{-6}cm)	5.9[11]	17.	1.8
m	Molecular Weight		29.0[12]	4.00[12]	170.9[14]

a) at 1 atm $\approx 10^6$ dynes/cm^2 $\approx$ 760 mm Hg

b) at $70^\circ F \approx 20^\circ C$

low pressures. As one expects from the theory, the effect of B decreases with increasing pressure; for high enough pressures, the loss factor is practically independent of B.

The test data (e.g., Fig. 6c, which corresponds to Fig. 5) show no pronounced peaks, and appear on the whole to agree best with the theoretical curves for B≈1. There is some disagreement at low pressures, where the theoretical curve for B=1 has a steeper slope than that generally indicated by the data. However, the measured loss factors for low pressures are small, and therefore of questionable validity, since these loss factors are obtained from the difference between two measured values of nearly equal magnitude. Although Dimeff, Lane, and Coon[3] found better agreement for B=30, a value of B=1 is more nearly what one would expect on the basis of physical reasoning (since B=1 implies that transition from confined to open space behavior occurs if the mean free path is of the same magnitude as the gap width).

Theoretically Predicted Loss Factor of Test Panel; Experimental Data

The results of calculations, using B=1 and the appropriate test plate-and-beam assembly and gas parameters, are shown in Figs. 6 – 8, together with the corresponding test data. Figure 6 pertains to air, Fig. 7 to helium, and Fig. 8 to Freon 114. In order to present this information in easily interpretable form, the data and curves for each gas have been spread over four sheets (i.e., each figure has been divided into four pages).

Discussion

Agreement Between Theory and Experiment

Inspection of Figs. 6 – 8 reveals that the experimental data generally agree reasonably well with the theoretical predictions, both in terms of trends and in terms of magnitudes. (The data of Fig. 6 are found also to agree with similar previous data.[1,2])

Because experimental determination of gas-pumping loss factors involves taking the difference between two loss factor measurements, each of which is subject to some error, the loss factor data must be considered as rather imprecise. This lack of precision is particularly important for low pressure data, where the small gas-pumping damping contribution is computed from the difference between two nearly equal quantities. The difficulty of measuring such small air-pumping damping contributions has made it impossible to measure these contributions in some cases; in other cases the lack of precision at low pressures might account for some of the discrepancy between theory and experiment at low pressures.

It is to be noted that for the test panel $k_p d \approx 5.5$ at 500 cps, so that no significant effects of the rivets on the gas-pumping damping are expected to occur at frequencies above 500 cps.

The discrepancies between experimental data and theoretical predictions may be attributed not only to the aforementioned experimental inaccuracies, but also to shortcomings in the theory. Several assumptions were made in the development of the theory, for the sake of tractability. Among the most questionable of these are those concerned with the effect of the rivets, with

confining attention to plate waves impinging normally on the beam, and with fluid-structure interaction. It is, indeed, gratifying to note how well a relatively simple theory can predict the salient features of the observed behavior, in spite of the possibly marginal validity of some of these assumptions.

Similarity of Results for Different Gases

It is of interest to note that the theoretical calculations predict that all three gases used should produce very nearly the same gas-pumping loss factor contribution, in spite of their greatly differing kinematic viscosities. That this prediction is actually realized is evident for example from Fig. 9, which compares corresponding loss factor curves and data for all three gases at 1,000 cps and 8,000 cps.

This, at first glance, somewhat surprising very weak dependence on the character of the gas may be explained in part by the fact that at least for the gases used here, the gases with greater kinematic viscosities also had greater acoustic velocities (Table I). Thus, the more viscous gases presented greater stiffnesses to the plate motions, restricted the plate motions more, and hence were pumped to a lesser degree.

SUMMARY AND CONCLUSIONS

Summary

The foregoing results reinforce the previous finding[1,2] that the dissipation of vibratory energy at riveted (or other multi-point-fastened) joints between panels and relatively stiff reinforcing members (beams), at frequencies considerably higher than the panel fundamental, occurs primarily as a result of the gas "pumping" that is produced as adjacent surfaces of the panels and reinforcing members move away from and toward each other.

The induced oscillatory gas flow in the interspace between a panel and reinforcing beam is primarily tangential to the surfaces, and energy dissipation results from viscous losses in this flow.

The viscous losses in the oscillatory flow are confined essentially to boundary layer regions near the solid surfaces. The thickness of such a region is proportional to the square-root of the kinematic viscosity of the gas in the plate-beam interspace, and inversely proportional to the square-root of frequency. If the boundary layer thickness is much smaller than the interspace gap thickness, then only a small fraction of the gas in the interspace participates effectively in the energy dissipation, and relatively little damping results. On the other hand, if the boundary layer thickness is much greater than the gap thickness, then all of the gas participates in the dissipation, but viscous forces greatly restrict its motion, so that the total energy dissipation again is small. Maximum energy dissipation occurs at an intermediate condition, where the boundary layer thickness is roughly half of the gap thickness.

The amount of gas pumping that is produced by a given panel vibration, and thus the magnitude of the gas-pumping damping, also depends on the ratio of the "local stiffness" of the gas in the interspace to the "local mass" of the panel. This ratio increases with increasing ambient pressure and with decreasing gap thickness and frequency. If this ratio is large, then the gas pressure in the interspace restricts the relative motion there, and there results comparatively little gas flow, and thus relatively little corresponding energy dissipation.

Two properties of the gas affect the gas-pumping loss factor that is obtained with a given structural configuration, at a given frequency, and at a given temperature and pressure. These properties are the kinematic viscosity of the gas (which depends on both pressure and temperature) and the acoustic velocity in the gas (which essentially depends only on temperature). However, at low pressures, where the molecular mean free path is larger than the gap thickness, the kinematic viscosity differs from the usual "large volume" value, and then also depends on the ratio of gap thickness to mean free path.

Concluding Remarks

Since it has been found that the gas-pumping mechanism may be responsible for a major portion of the total damping of a structure in air, and since gas-pumping damping decreases with decreasing ambient pressure, it is evident that vibration testing of aerospace structures at ground level atmospheric pressures may be unconservative. In such ground level tests the total structural damping is greater than that in rarefied atmosphere; thus, the vibration levels one measures in ground test may be significantly smaller than those one may encounter at reduced pressures (at altitude or outside the atmosphere) due to the same excitation.

Therefore it appears imperative to test critical aerospace structures or components under vacuum conditions, or to subject them at atmospheric pressures to appropriately higher excitation levels in order to take the reduced damping in vacuum into account.

Although it is hoped that the study presented in this report supplies a step toward the understanding of the gas-pumping damping mechanism, much work remains to be done.

It is important to reiterate that the analysis presented in this report deals only with frequencies that are much higher than the panel fundamental at which the plate flexural wavelengths exceed the distances between adjacent rivets or bolts. Thus, the present analysis does not deal with bellows-like gas-pumping-damping produced by gross to-and-fro relative motion between two structural components. However, now that the groundwork has been laid, one should be able to perform analyses of the important lower-frequency problems relatively directly.

The present analysis is a greatly simplified one, as has been mentioned, and therefore suffers several shortcomings. Extensions of the theory to take better account of such items as the action of the rivets, of the finite beam mass and stiffness, and of the gas-structure interaction, would be useful.

Additional measurements, to determine whether predicted temperature-dependences are realized, are indicated in order to explore the validity of the developed theory more fully. A study of gas-pumping damping of a practical structure under realistic conditions, and of optimization of this damping, may be expected to be both useful and instructive.

Acknowledgement

The authors are indebted to Mr. J.R. Carbonell, who contributed significantly to the reported work in its initial stages, and to Mr. C.W. Vest, who carried out most of the experimental measurements. A condensed form of the analytical portion of this report appears in Ref. 15, an early draft of which has served as a basis for preparation of the present report.

REFERENCES

1. Ungar, E.E.: Energy Dissipation at Structural Joints; Mechanisms and Magnitudes. U.S. Air Force Flight Dynamics Laboratory, FDL-TDR 64-98, July 1964.

2. Ungar, E.E.; and Carbonell, J.R.: On Panel Vibration Damping Due to Structural Joints. AIAA J., Vol. 4, Aug. 1966, pp. 1385-1390.

3. Dimeff, J.; Lane, J.W.; and Coon, C.W.: New Pressure Transducer. Rev. Sci. Instr., Vol. 33, 1962, p. 804.

4. Ungar, E.E.; and Kerwin, E.M., Jr.: Loss Factors of Viscoelastic Systems in Terms of Energy Concepts. J. Acoust. Soc. Am., Vol. 34, July 1962, pp. 954-957.

5. Landau, L.D.; and Lifshitz, E.M.: Fluid Mechanics. Pergamon Press, London, 1959. Chapters I, II; pp. 54, 2, 49, 24, 63, 89.

6. Maidanik, G.: Response of Ribbed Panels to Reverberant Acoustic Fields. J. Acoust. Soc. Am., Vol. 31, 1962, pp. 809-826.

7. Kurtze, G.: Bending Wave Propagation in Multilayer Plates. J. Acoust. Soc. Am., Vol. 31, 1959, pp. 1183-1201.

8. Heckl, M.: Compendium of Impedance Formulas. Bolt Beranek and Newman Inc. Rept. No. 774, 1961.

9. Smith, P.W., Jr.: Coupling of Sound and Panel Vibration Below the Critical Frequency. J. Acoust. Soc. Am., Vol. 36, 1964, pp. 1516-1520.

10. Plunkett, R.: Measurement of Damping. Sec. 5 of Structural Damping, J. Ruzicka, ed., Am. Soc. Mech. Engineers, New York, 1959.

11. Jeans, J.H.: The Dynamical Theory of Gases, Fourth ed., Dover Publications, Inc., 1954.

12. McAdams, H.W.: Heat Transmission, Second ed., McGraw-Hill Book Co., Inc., 1942, pp. 410, 411.

13. Obert, E.F.: Thermodynamics, McGraw-Hill Book Co., Inc., 1948, p. 541.

14. Freon Technical Bulletin B-2, E.I. duPont de Nemours and Co., "Freon" Products Division.

15. Maidanik, G.: Energy Dissipation Associated with Gas-Pumping in Structural Joints. J. Acoust. Soc. Am., Vol. 40, 1966, pp. 1064-1072.

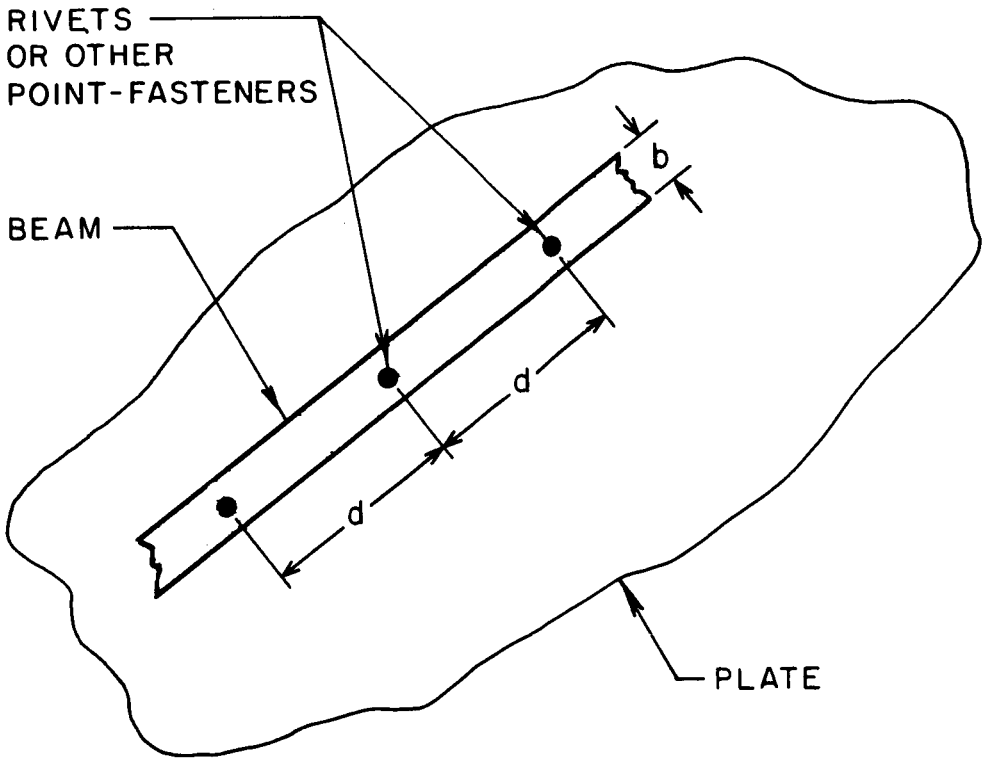

FIG. 1 PLATE WITH MULTI-POINT-FASTENED ATTACHED BEAM

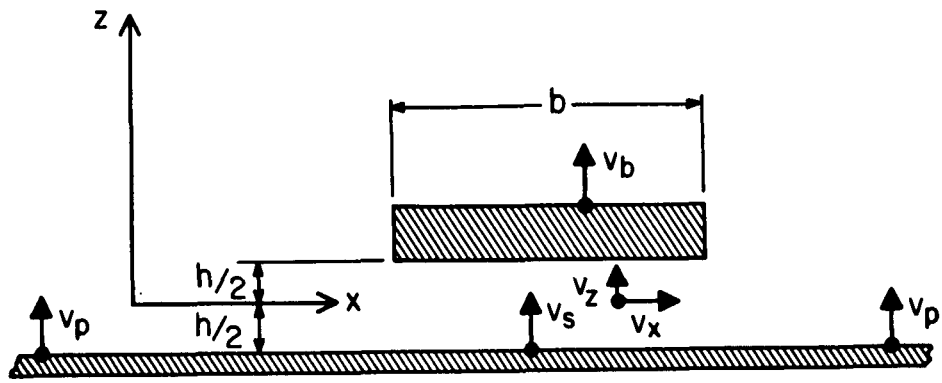

FIG. 2 GEOMETRY AND COORDINATES OF SECTION TAKEN THROUGH PLATE PERPENDICULAR TO BEAM LENGTH

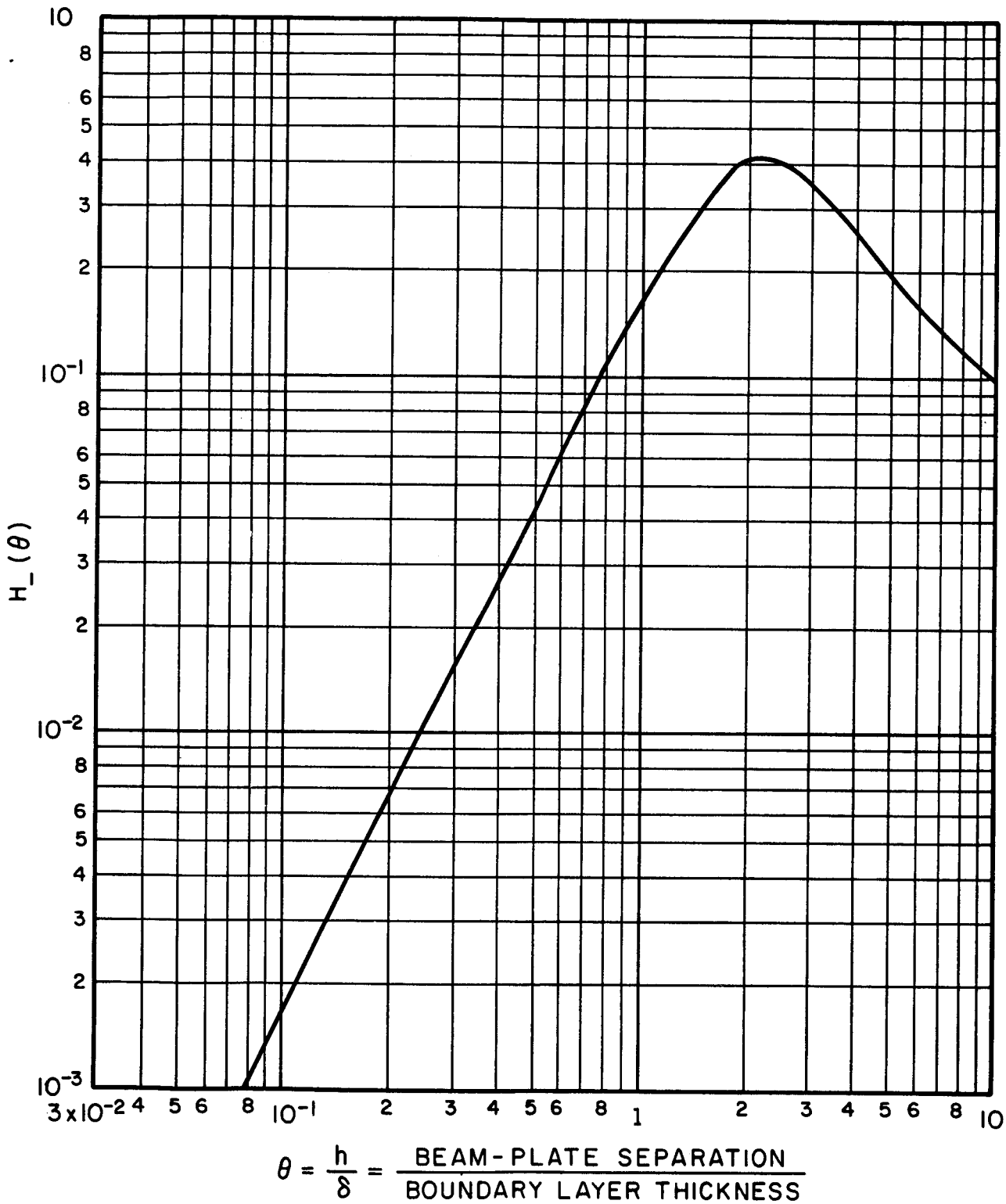

FIG. 3 THE FUNCTION $H_-(\theta)$

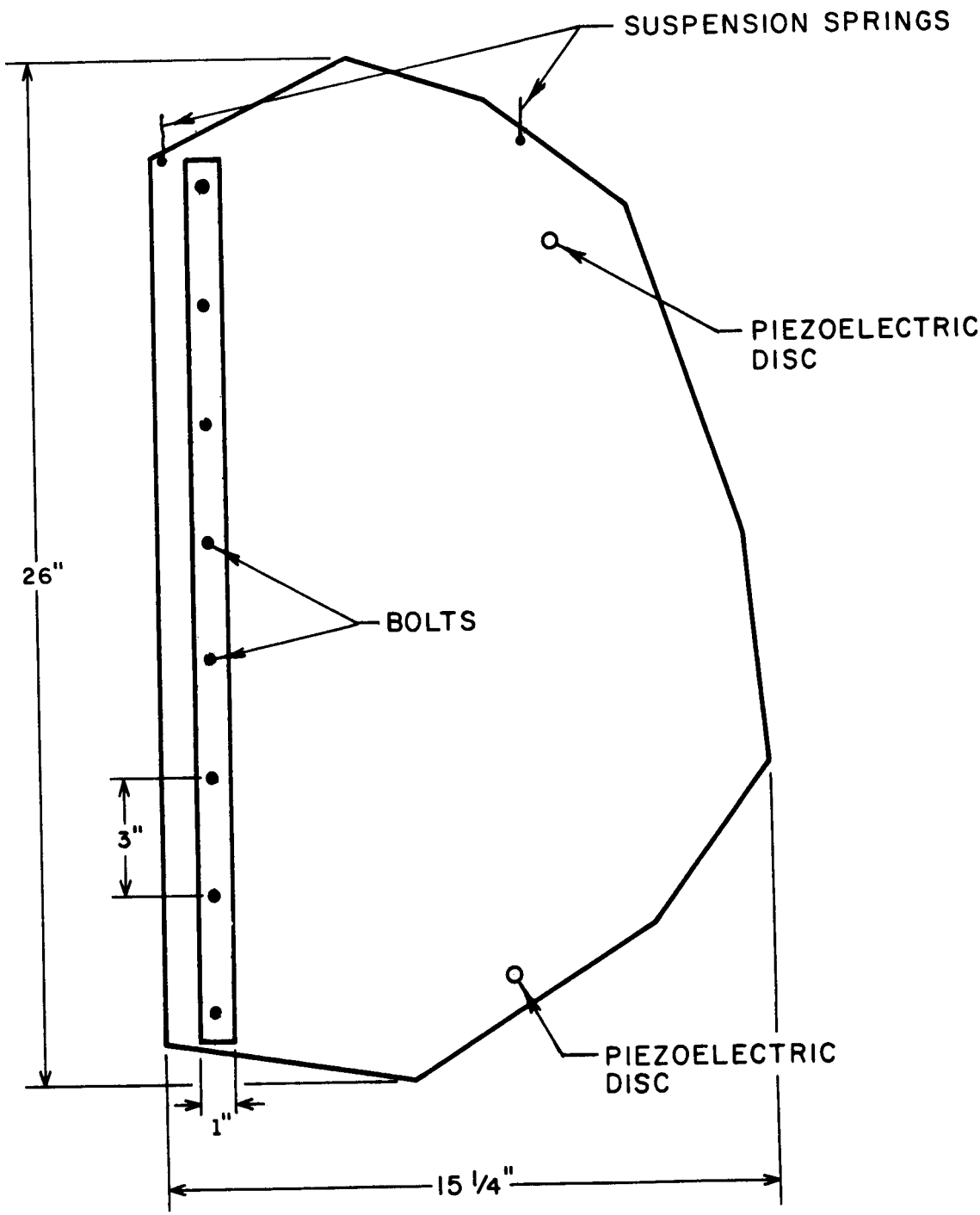

FIG. 4 TEST PANEL (SHOWN APPROXIMATELY 1/4 SCALE)

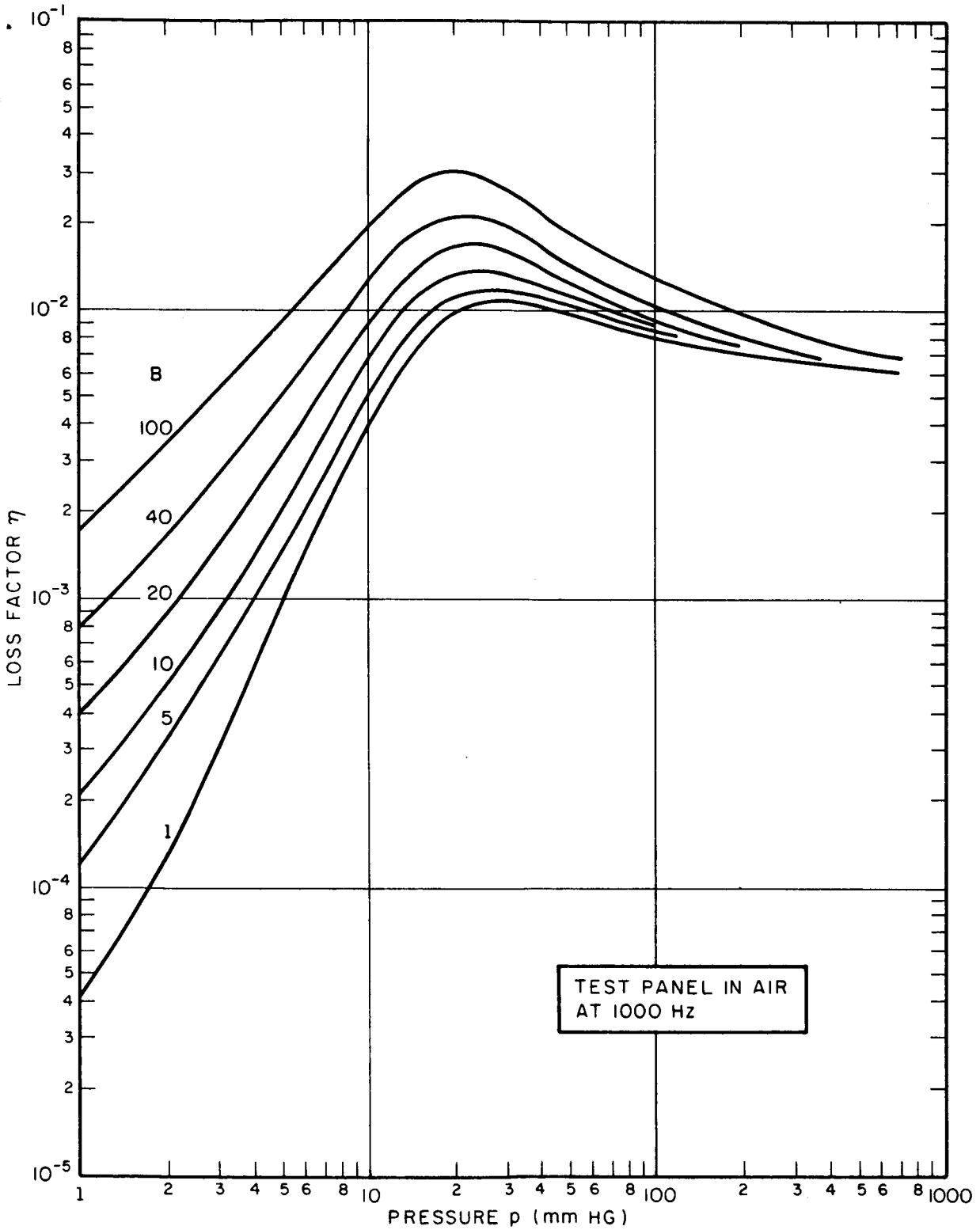

FIG. 5 DEPENDENCE OF THEORETICAL GAS-PUMPING LOSS FACTOR ON TRANSITION PARAMETER B

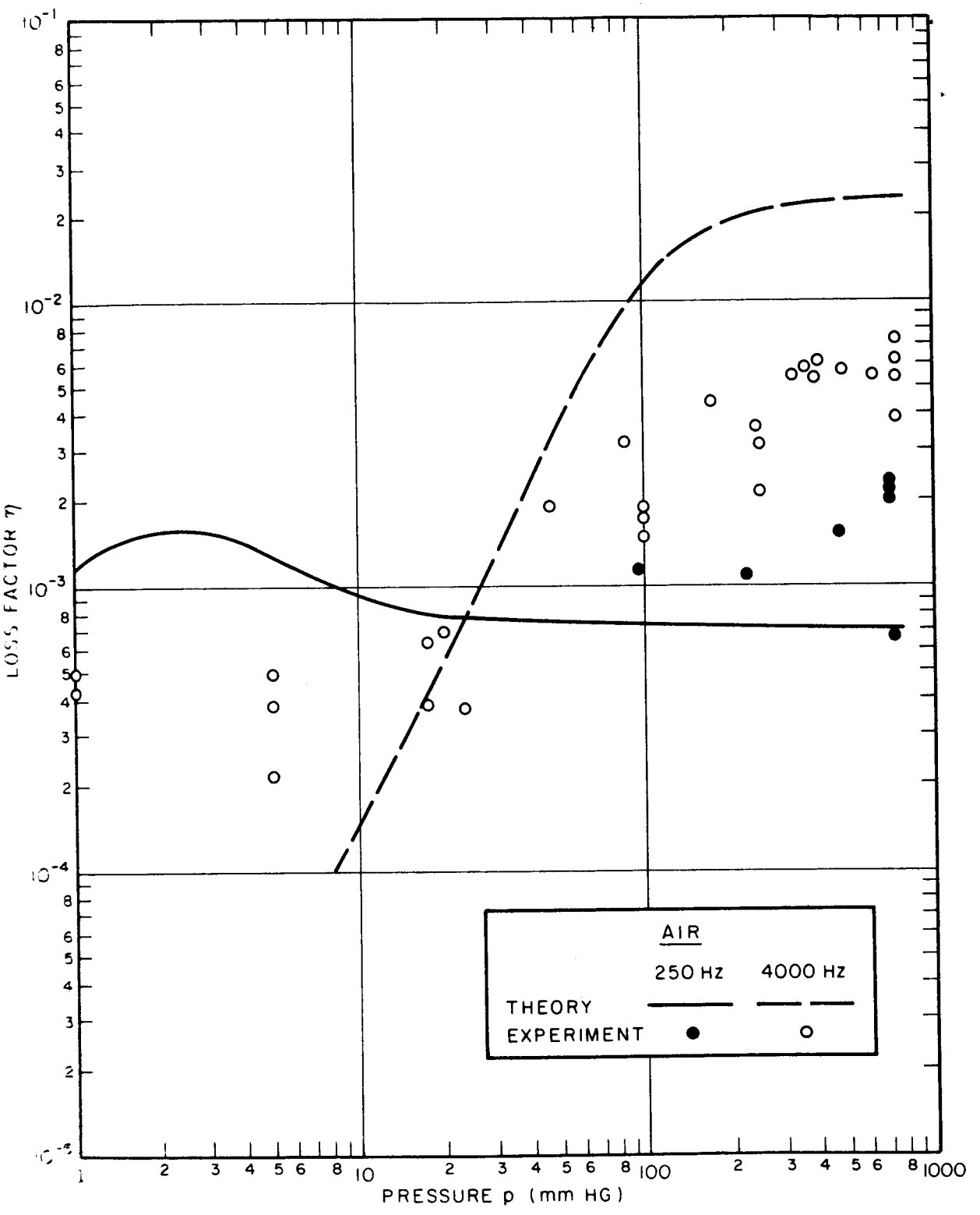

FIG. 6a GAS-PUMPING LOSS FACTOR OF TEST PANEL IN AIR AT 250 AND 4000 Hz

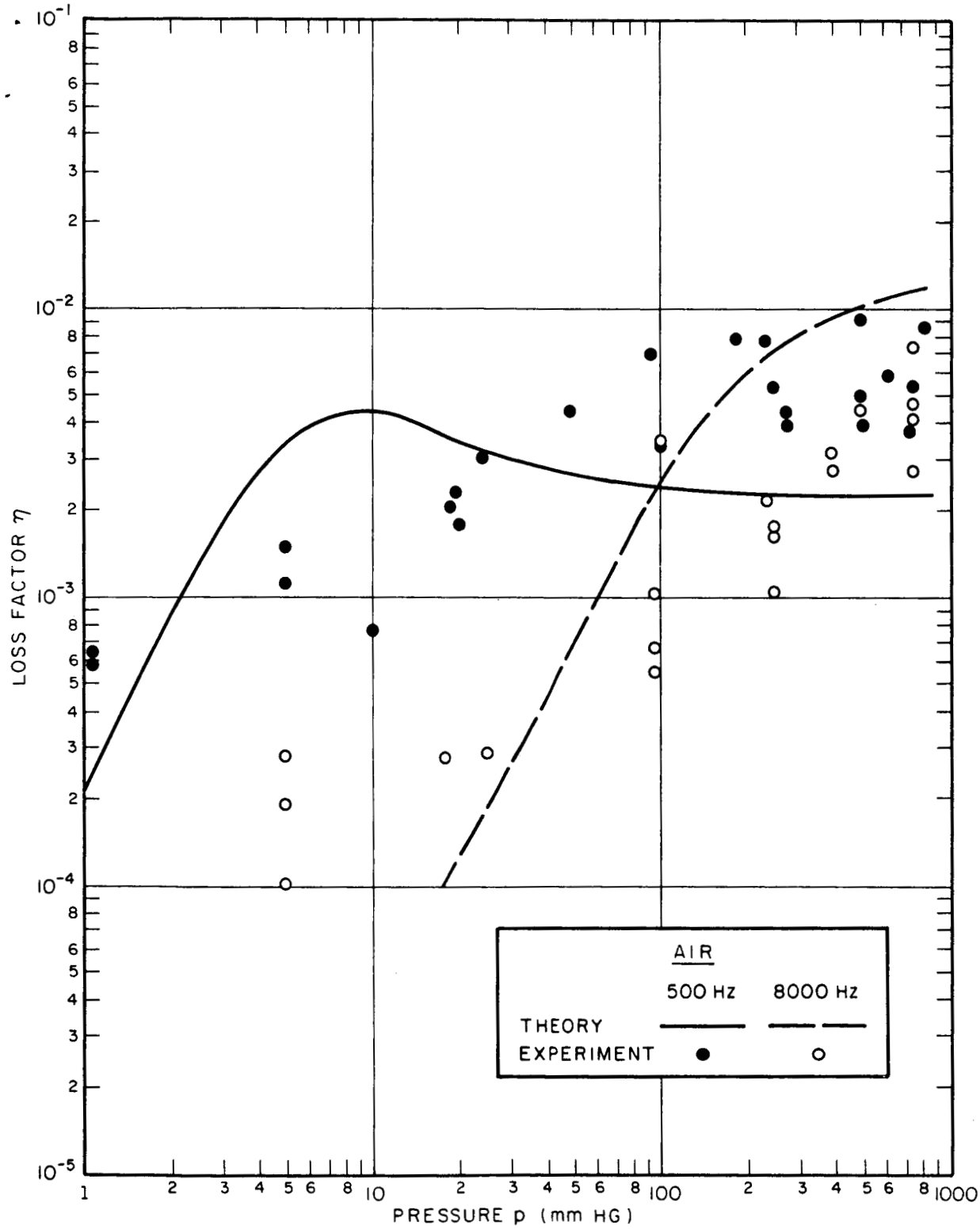

FIG. 6b GAS-PUMPING LOSS FACTOR OF TEST PANEL IN AIR AT 500 AND 8000 Hz

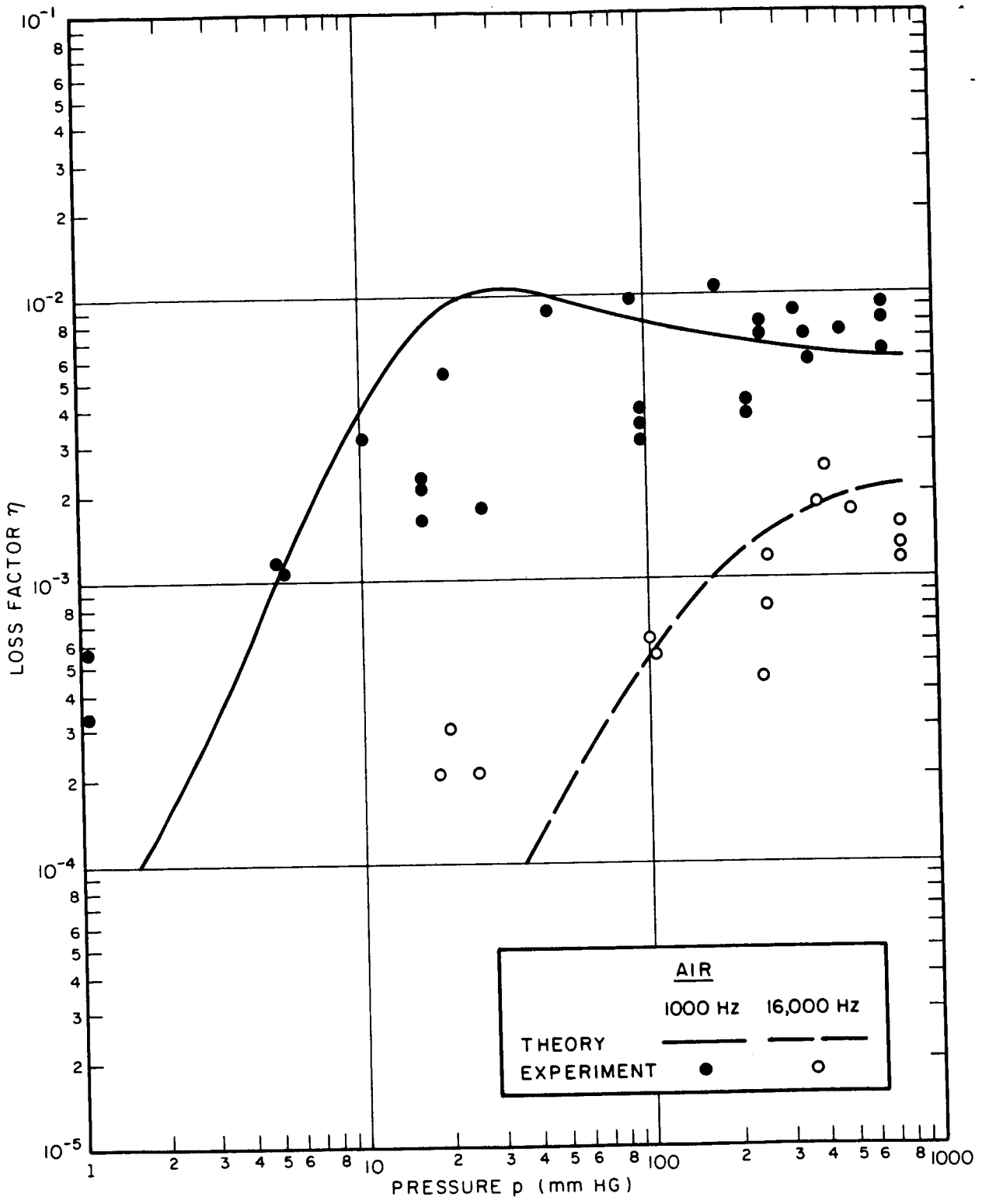

FIG. 6c GAS-PUMPING LOSS FACTOR OF TEST PANEL IN AIR AT 1000 AND 16,000 Hz

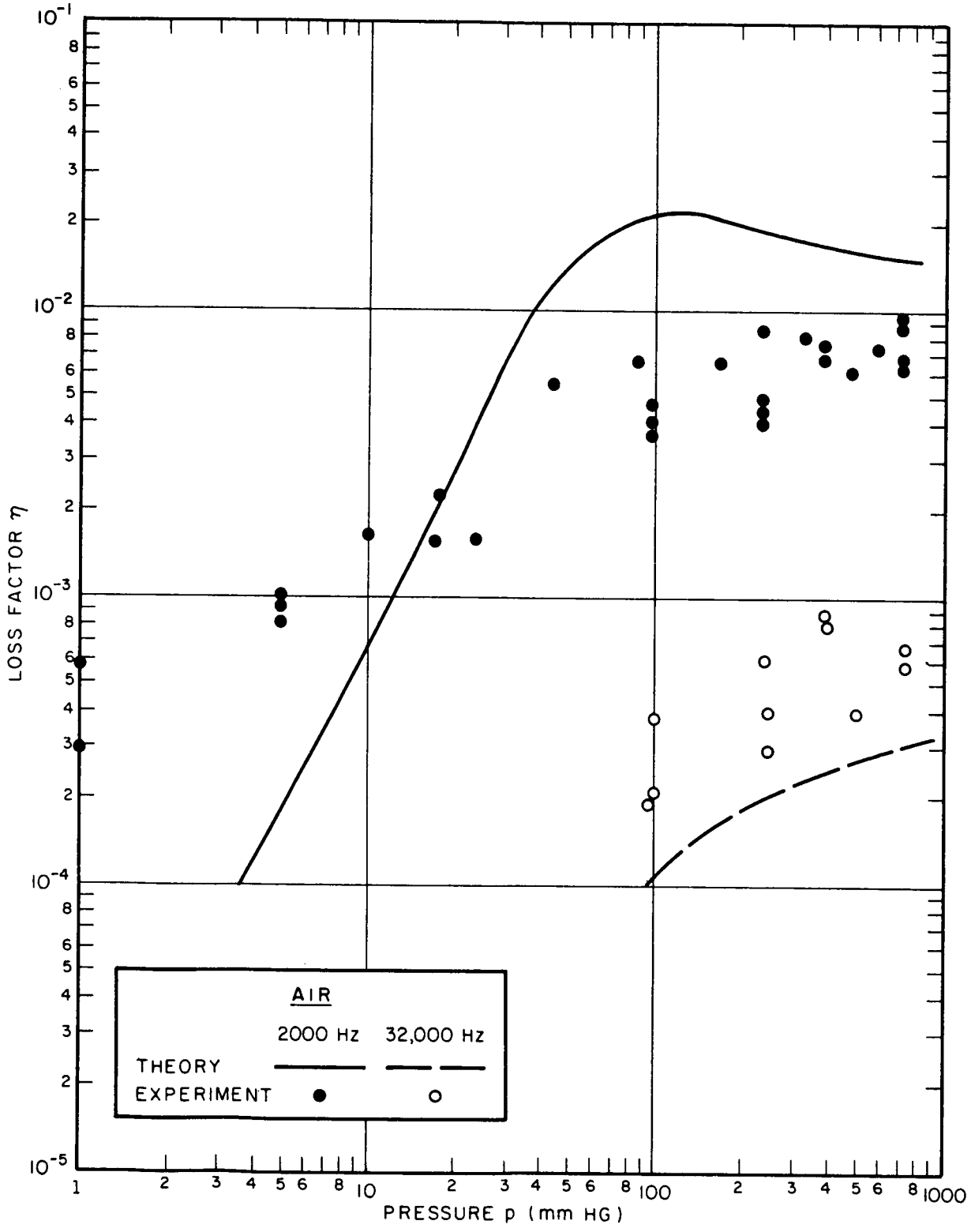

FIG. 6d GAS-PUMPING LOSS FACTOR OF TEST PANEL IN AIR AT 2000 AND 32,000 Hz

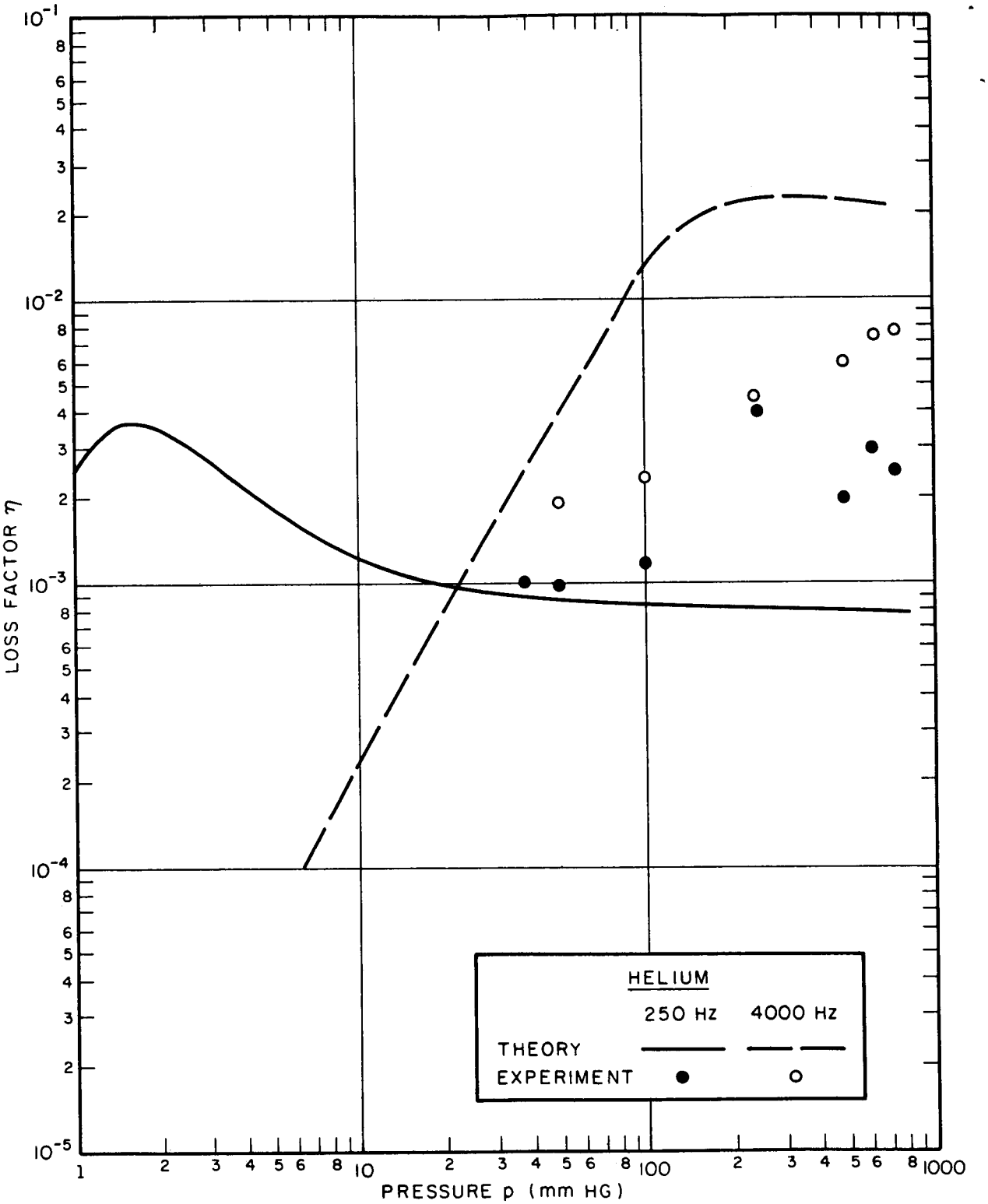

FIG. 7a GAS-PUMPING LOSS FACTOR OF TEST PANEL IN HELIUM AT 250 AND 4000 Hz

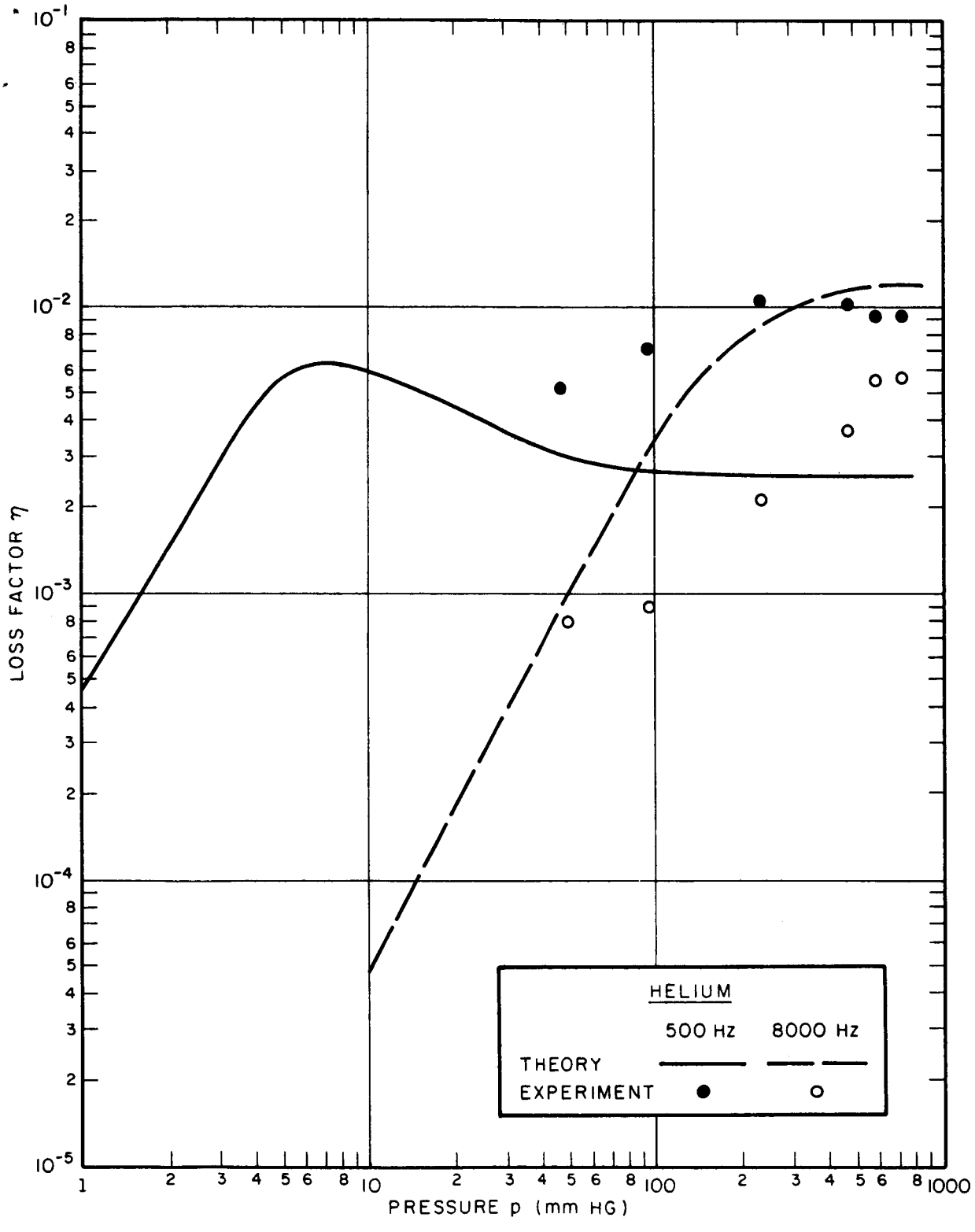

FIG. 7b GAS-PUMPING LOSS FACTOR OF TEST PANEL IN HELIUM AT 500 AND 8000 Hz

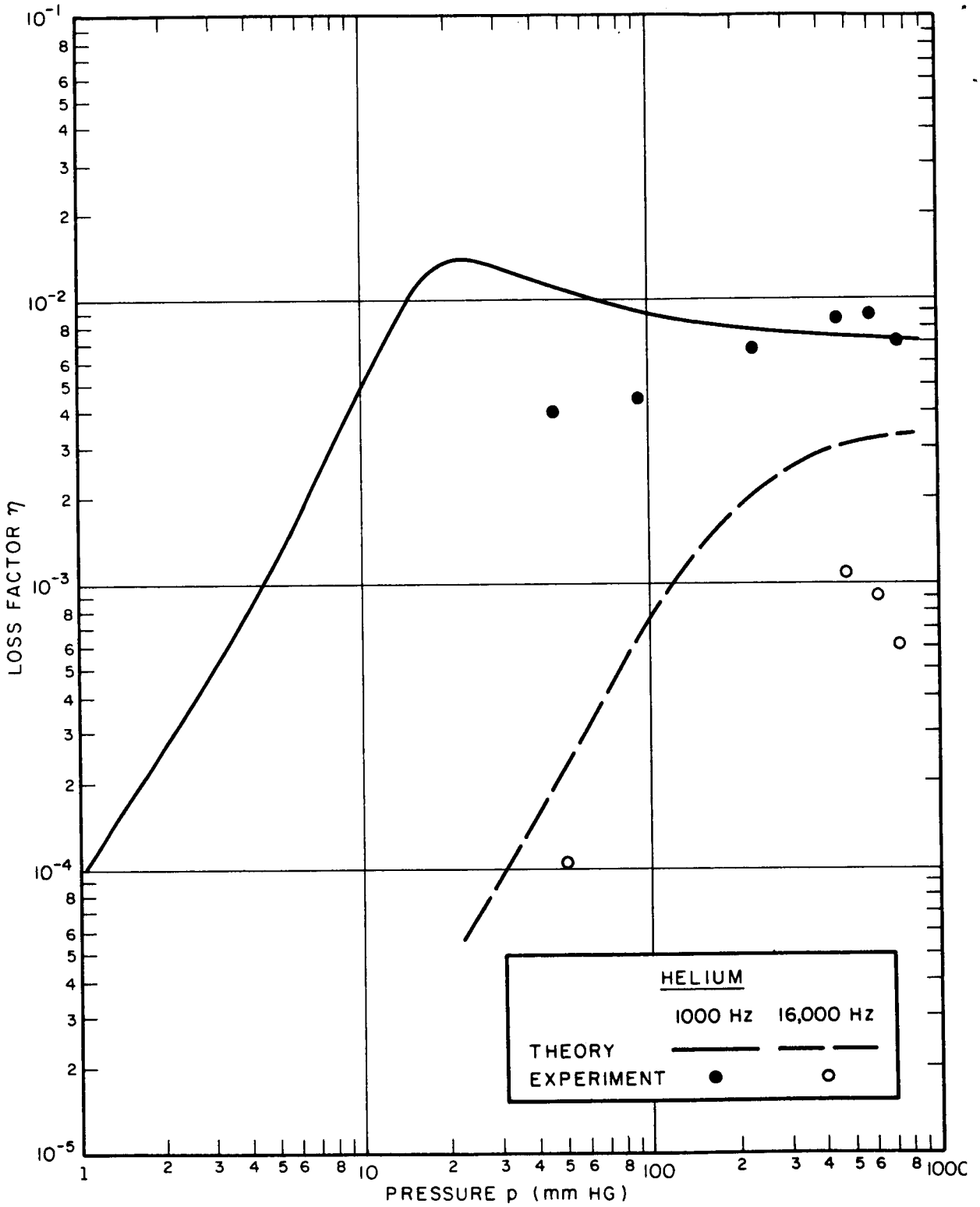

FIG. 7c GAS-PUMPING LOSS FACTOR OF TEST PANEL IN HELIUM AT 1000 AND 16,000 Hz

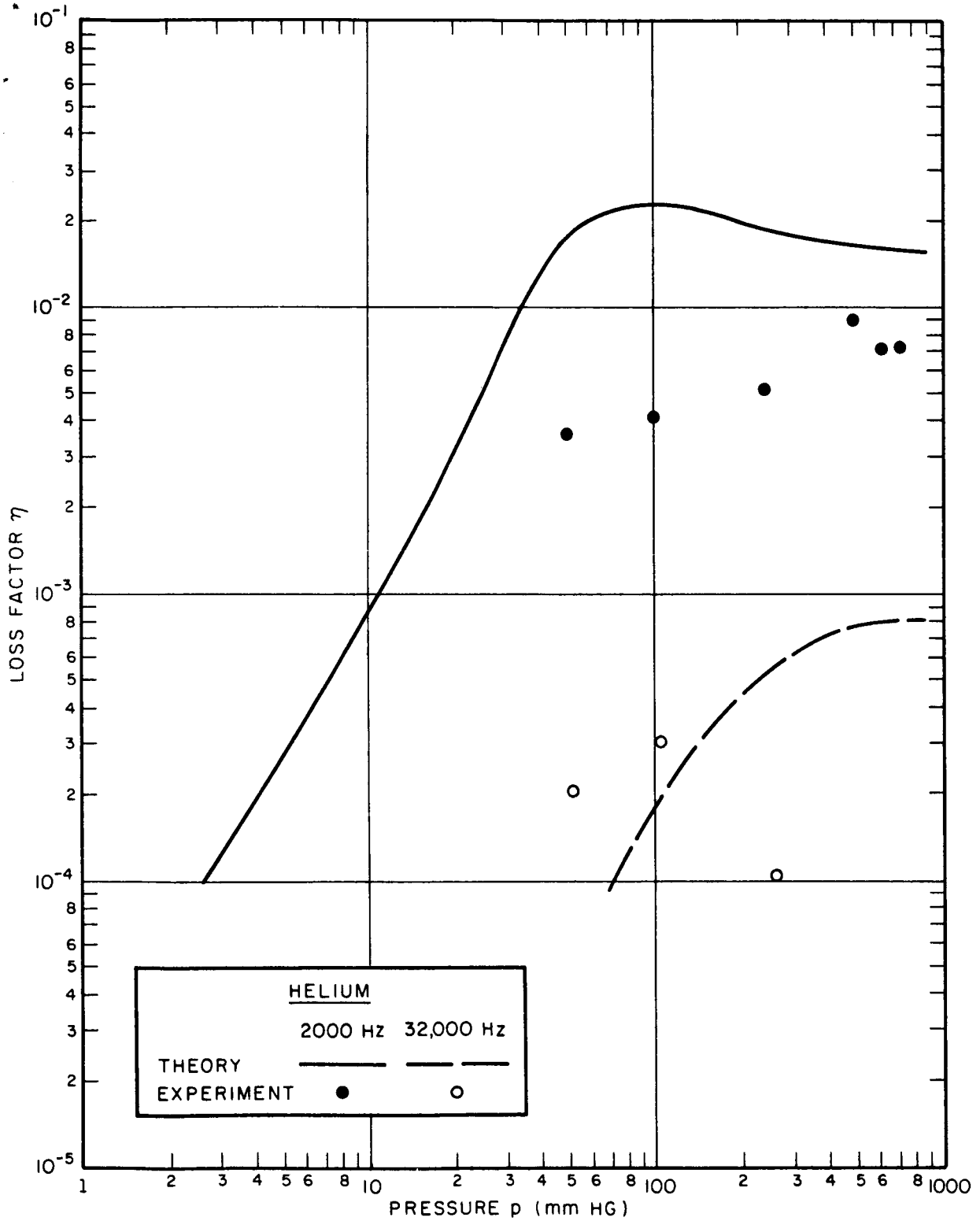

FIG. 7d GAS-PUMPING LOSS FACTOR OF TEST PANEL IN HELIUM AT 2000 AND 32,000 Hz

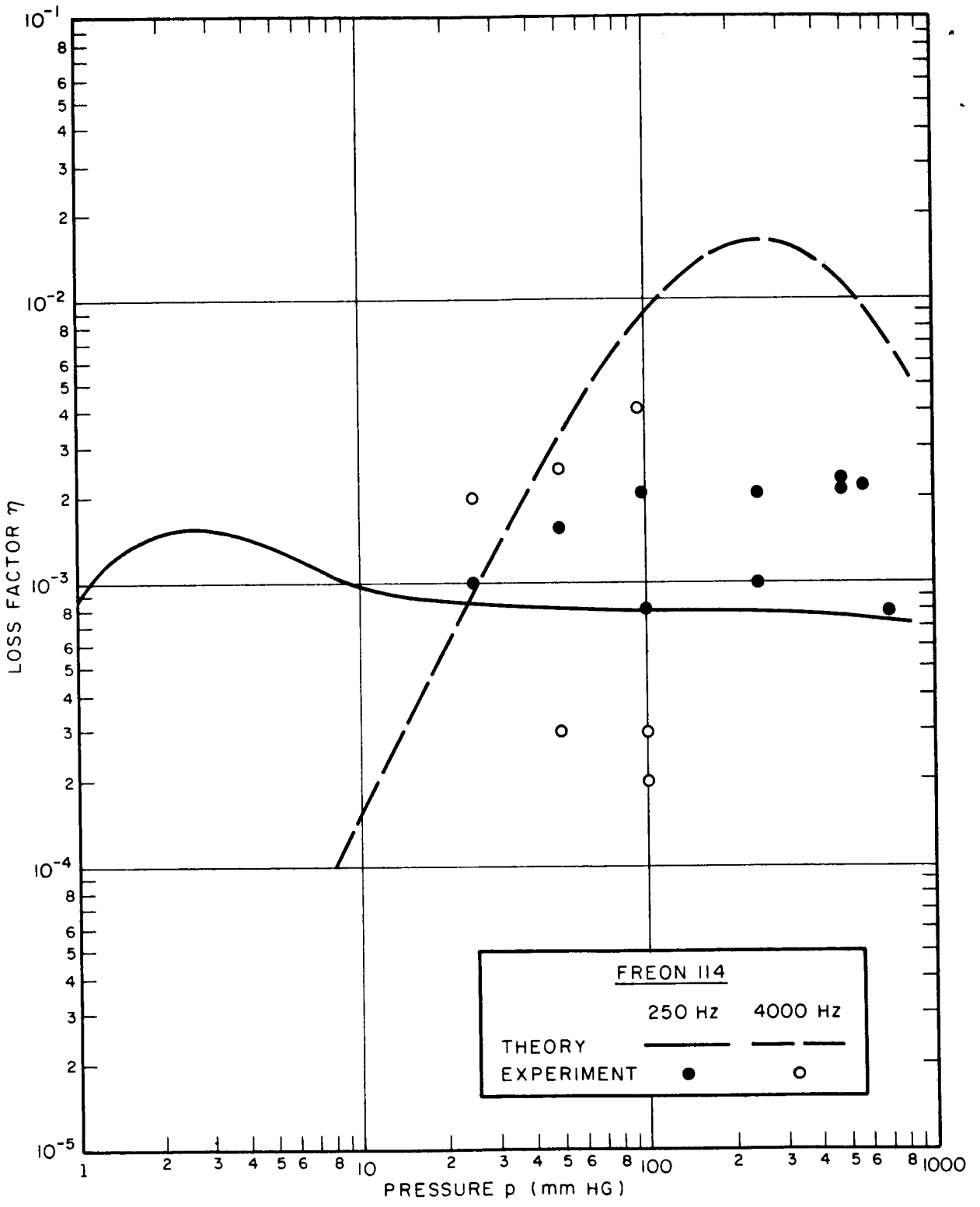

FIG. 8a GAS-PUMPING LOSS FACTOR OF TEST PANEL IN FREON 114 AT 250 AND 4000 Hz

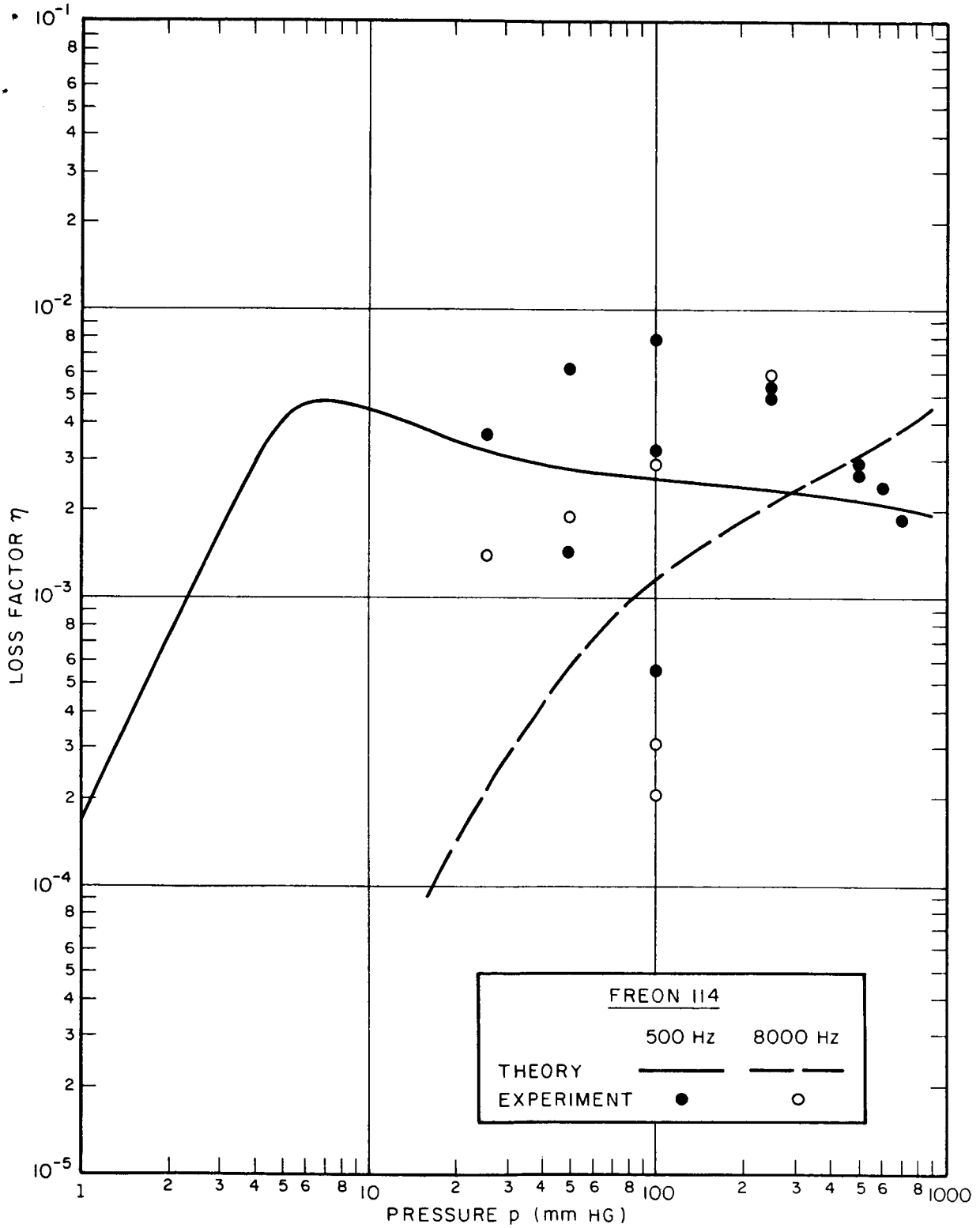

FIG. 8b GAS-PUMPING LOSS FACTOR OF TEST PANEL IN FREON 114 AT 500 AND 8000 Hz

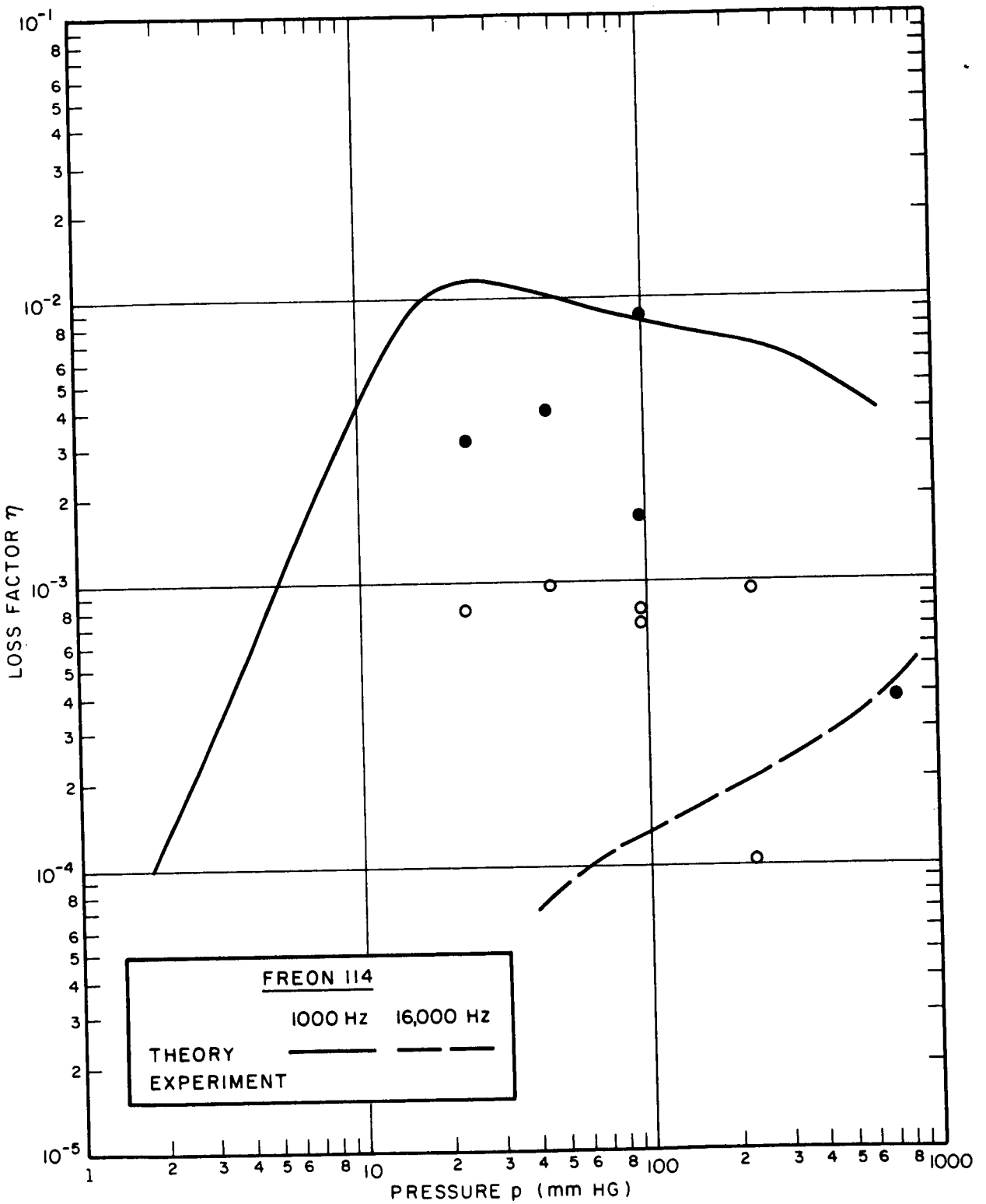

FIG. 8c GAS-PUMPING LOSS FACTOR OF TEST PANEL IN FREON 114 AT 1000 AND 16,000 Hz

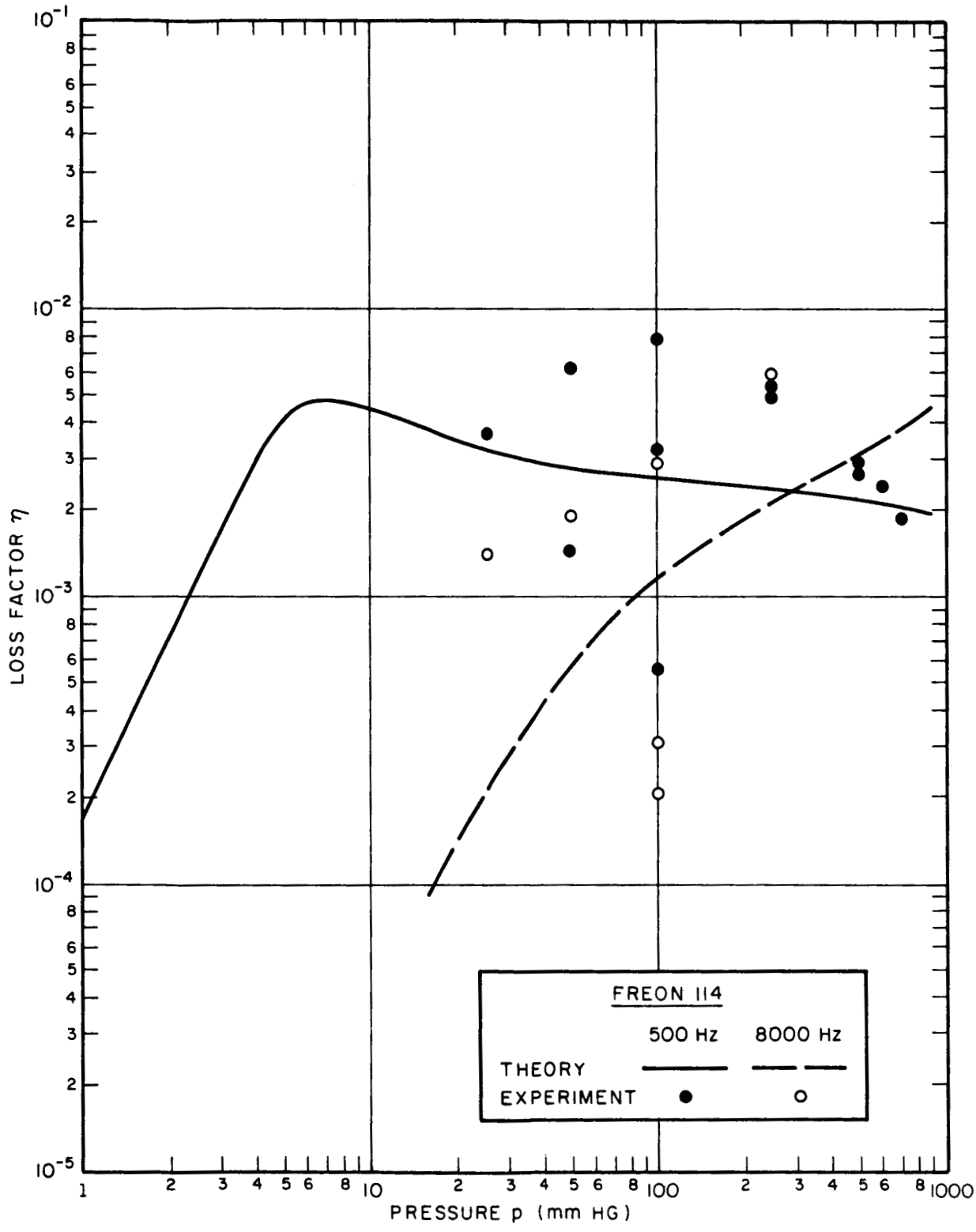

FIG. 8d GAS-PUMPING LOSS FACTOR OF TEST PANEL IN FREON 114 AT 2000 AND 32,000 Hz

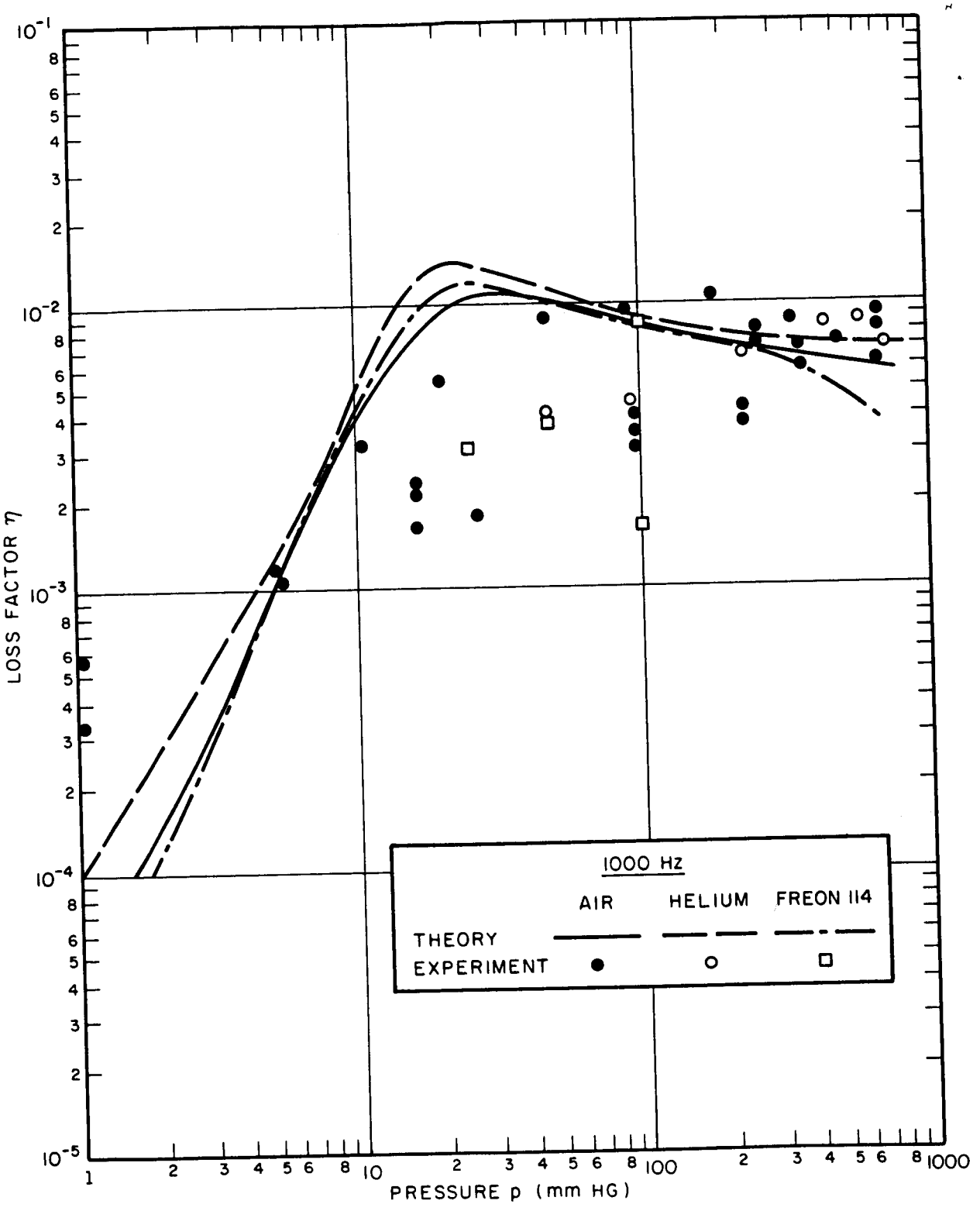

FIG. 9a GAS-PUMPING LOSS FACTOR OF TEST PANEL IN THREE DIFFERENT GASES AT 1000 Hz

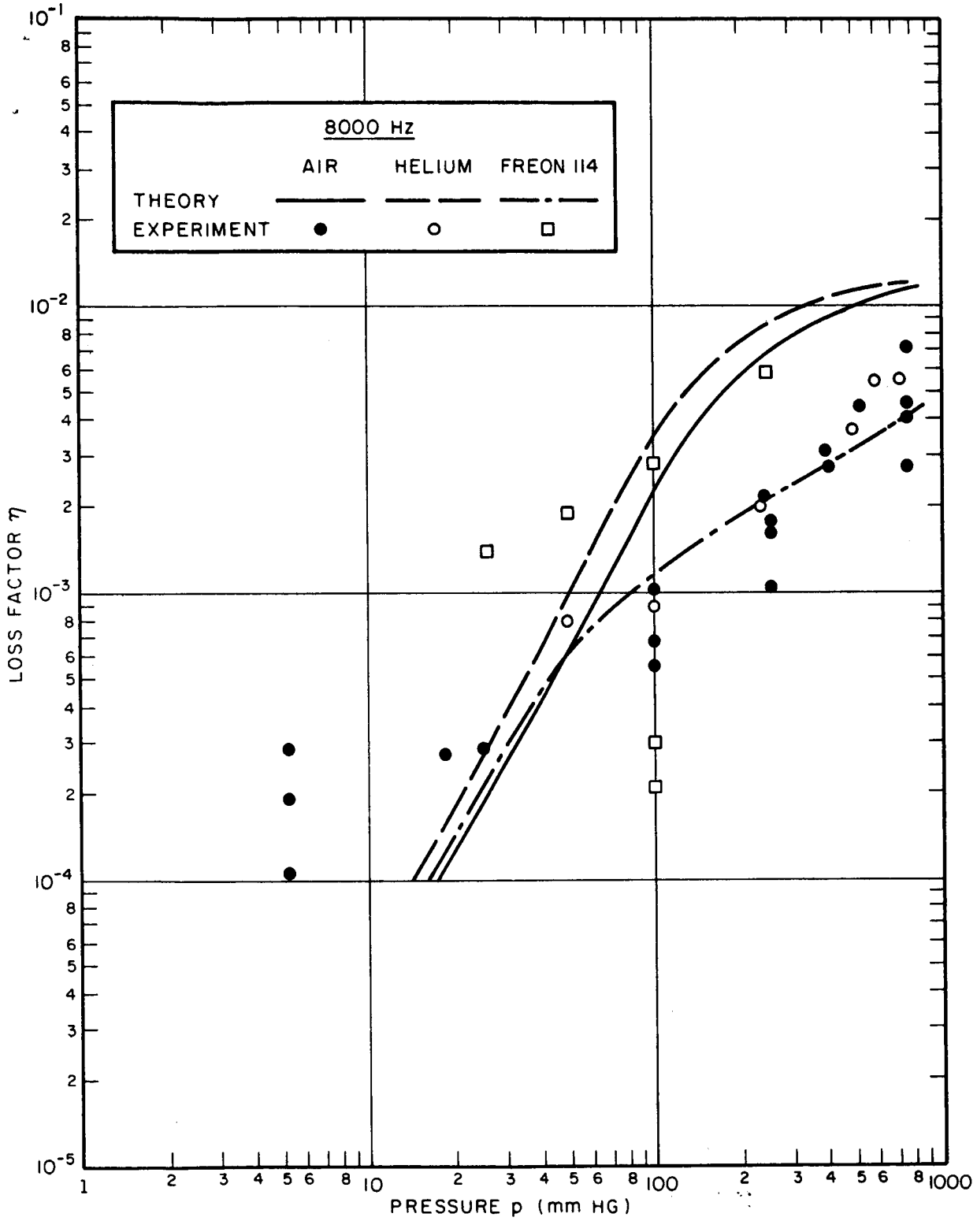

FIG. 9b GAS-PUMPING LOSS FACTOR OF TEST PANEL IN THREE DIFFERENT GASES AT 8000 Hz